DRYING CHARACTERISTICS OF RAMIE FIBER

A THESIS

Presented to

the Faculty of the Division of Graduate Studies

Georgia Institute of Technology

In Partial Fulfillment

of the Requirements for the Degree

Master of Science in Chemical Engineering

by

John Lewis Hancock

May 1949

DRYING CHARACTERISTICS OF RAMIE FIBER

Approved:

J. M. Dalrymple

James L. Taylor

Wm. Meese Newton

Date Approved by Chairman _____*May 17, 1959*_____

TABLE OF CONTENTS

LIST OF TABLES

	Title	Page

LIST OF FIGURES

DRYING CHARACTERISTICS OF
RAMIE FIBER

SUMMARY

This study was undertaken to obtain data that would permit an analysis of the mechanism and characteristics of the adiabatic drying of garnetted ramie fiber.

Equilibrium moisture was determined for several points in order to check that available in the literature (34). Rate of drying studies were made at 140 °F, 170 °F, and 200 °F, at relative humidities from 1% to 51%, at air velocities from 500 ft/min to 1050 ft/min, at dry densities from 0.110 fm/cc to 0.232 gm/cc upon slabs of degummed garnetted ramie from 0.635 cm to 2.54 cm thick. The results were plotted and analyzed. The results and their graphical analysis are presented in Figs. 1 through 21.

INTRODUCTION

Ramie is a bast fiber which is produced naturally in the bark of the stalk of the Boehmeria tenacisscina; China grass is produced naturally in the bark of the Boehmeria nivea, but they have never been distinguished in the economic literature (5). Ramie is the name commonly used to designate all "Boehmeria" fiber; and China grass is a synonym and trade name of the fiber imported from China.

The plant is found in India, China, Haiti, Japan, Southern Europe, the Southern United States, Hawaii, and other countries located in tropical or sub-tropical climates. The plants generally grow five to eight feet high and are cut upon reaching maturity (2). The stalk is usually decorticated while green. The process has been one of the major obstacles in the successful treatment of the fiber. In the Orient the decortication is carried out by hand, but the limited productivity of this method restricts it to areas where labor is cheap and plentiful. Experimenters in the United States have recently developed a machine which is reported to perform the operation satisfactorily (19).

The presence of chemical gums causes the decorticated fiber to become stiff when dry. These gums, which are principally cutose, vasculose, and pectose, must be completely removed before the fiber can be utilized as a textile. The first two can be easily dissolved with soap and alkalies under pressure, after which the pectose can be removed by washing (2). The fiber is then ready for the garnetting process.

The literature with one exception (34) reveals no data on the drying of ramie fiber, and reveals none whatever that may be used in determining the mechanism of drying. Furthermore the literature

reveals no data on the drying of cotton or other similiar fibers which may be used to analyze the mechanism of the drying of fibers in general. The need for such data and their analysis is present in all textile industries requiring a drying operation, and is becoming increasingly important for ramie as a result of success obtained by research in other phases of processing.

It is the purpose of this study to obtain data that can be analyzed to determine the mechanism and characteristics of drying of ramie fiber, and fibers in general, that will be useful in designing drying equipment and processes.

OBJECT

One part of this investigation was to check existing equilibrium data on degummed garnetted ramie fiber. Several points were checked by determining equilibrium moisture content at 140 °F, 170 °F, and 200 °F as a function of relative humidities of 19%, 33%, and 51% of the enclosing atmosphere.

The other part of this investigation was to determine the drying mechanism and characteristics of degummed garretted ramie. Drying rates were obtained and analyzed at 140 °F, 170 °F, and 200 °F, at relative humidities of 19% to 51%, at air velocities of 500 ft/min to 1050 ft/min, at densities from 0.110 gm/cc to 0.232 gm/cc upon slabs of ramie from 0.635 cm to 2.54 cm thick.

EXPERIMENTAL EQUIPMENT

The basic piece of experimental equipment was a Proctor-Schwartz laboratory dryer. See Diagrams 1 and 2 in the Appendix. This dryer is of a compartment-tray design heated by a Trane steam heater. The drying compartment measures 24x24x48 inches. The necessary humidification is supplied by an open steam humidifier and an air-water spray. Baffling arrangements and dampers on either side of the drying compartment permit three methods of air circulation and variable recirculation.

The temperature and relative humidity in the dryer are regulated by a Foxboro wet and dry bulb recorder-controller. The wet bulb is of the porous sleeve type. The controller is air operated employing dual controls; one control system governs the dry bulb temperature, and the other the wet bulb temperature.

Air is circulated through the dryer by a #3LLD Buffalo fan driven by a one and a half horsepower Diehl motor connected to the blower through a variable speed drive. The arrangement permits fan speeds of 274 to 1096 rpm.

Mounted on top of the dryer is a Toledo scale equipped with a hook which is suspended in the drying compartment. The scale is furnished with one ten pound blank beam, two ten pound beams with one ounce gradations and a five pound chart with one one hundredth of a pound calibrations. This scale was not sensitive enough to weigh the slabs used in this study; so a O'Haus balance graduated in tenths of a gram with a capacity of five hundred grams was used instead.

A set of two calibrated brass tubes five-sixteenths inches in diameter spaced one and a half inches apart, one with a one one sixty-

fourth of an inch in diameter hole on the upstream side and the other with a similiar hole on the downstream side were used to measure air velocity. These tubes were connected to a draft guage filled with ethyl alcohol located outside the dryer by two rubber tubes. The tubes were calibrated against a pitot tube in a wind tunnel to determine the factor for the tubes (7). See Appendix for calibration data.

Other equipment used in the work included an analytical balance, open air electric furnaces, and the usual laboratory equipment.

EXPERIMENTAL PROCEDURE

The fibers used in the investigation were processed as described in the Appendix. To insure uniformity of the samples, all studies were made on specimens of one processing.

The experimental work necessary to obtain equilibrium moisture check data was performed first. For every run four samples of the fiber were prepared by securing them with a short piece of stainless chrome wire. Two of these samples were placed in an open air electric oven and dried at least six hours at a temperature of 200 °F to bring the moisture content below the equilibrium value for the conditions of the run[1]. The other two samples were placed in tap water and allowed to soak at least six hours to thoroughly saturate the fiber.

The Proctor-Schwartz dryer was used as a constant atmosphere bath. The temperature and relative humidity for the run were established with complete recirculation of the air at a low air velocity. The four samples were then suspended in the air stream and allowed to remain at least thirty-six hours. This time has been proven to be sufficient time to insure equilibrium between the samples and the air (9)(34).

After thirty-six hours the samples were moved quickly to numbered 250 ml Erlenmeyer flasks, which were then tightly closed with rubber stoppers. The flask containing the samples were weighed on an analytical balance. The samples were then removed from the flasks and

[1]A few fine free fibers on the surface of the ramie samples charred slightly at this temperature. A few determinations were made at 150-60°F, where no charring occurs, and it was discovered that the amount charred was so small as to not affect the bone dry weight.

placed in the open air electric oven. The samples were dried at 200 $^\circ$F for twenty-four hours which brought them to a bone dry condition. This time has been proven to be sufficient to reach a constant weight (34).

Next each sample was replaced in its original flask and reweighed on the analytical balance. The sample was then discarded and the flask, stopper, and wire that bound the sample were weighed to determine the tare weight. The three weights give sufficient information to determine the equilibrium moisture content.

The rate of drying studies were made last. A slab of ramie was made by packing the fibers to the desired density in a rectangular frame eight by five inches made of one thirty-second inch brass strip of the desired width to give proper slab thickness. The slab was held in position in the drying compartment by four pieces of small stainless chrome wire attached to a hook. Drying from the edges of the slab was prevented by the brass strip. Drying from the two surfaces of the slab was accelerated in the immediate vicinity of the brass strip due to the high heat conductivity of the brass, but this effect was small and introduced an error that was constant.

Considerable trouble was experienced in obtaining a method of securing a uniform moisture distribution in the slab without air pockets prior to drying. Approximately twenty-five runs were made before a method of securing uniform moisture distribution and even packing that would give reproducible results was devised. The method finally used was to soak a weighed sample of ramie in tap water for six or more hours, beating and squeezing it several times to remove all air bubbles and pockets. The soaked ramie was then packed into the brass frame and pressed between two flat boards to form a slab with two

smooth surfaces. All water was allowed to run out that would while pressing the slab to the desired density and thickness. Care was taken not to destroy the uniform moisture distribution by draining from either end of the slab.

The controls of the dryer were set to give the desired value of temperature, relative humidity and air velocity. Approximately eight tenths of the drying air was recirculated. This was found to be sufficient to maintain a constant atmosphere and could be controlled by the controller more easily than with no air being recirculated. The dryer was allowed to run until the chosen conditions balanced out on automatic control. With the drying conditions thus equilibrated, the slab was then suspended in the drying compartment in a stream of air flowing parallel to the two surfaces of the slab. The slab was removed from the dryer and weighed on the O'Haus balance every five minutes. Exactly thirty seconds were allowed for weighing so that the slab actually dried in the dryer four and one half minutes between each reading. It was assumed no drying occured during the weighing process. Four and one half minutes was the time allowed for drying between each weighing in plotting and analyzing the data. This technique certainly is not the best, but is the best that could be devised with available equipment. The error introduced was made on each recording for each run, and had the effect of lowering the drying rates as the slab had to heat back up to the temperature of the drying atmosphere from room temperature after each weighing. Of course the amount of moisture lost while weighing compensated somewhat for the decreased drying rate immediately after each weighing. This is not as much as might be expected as there was little difference between the room temperature and the wet bulb temperature of the drying atmosphere

for most runs. The slab remains at the wet bulb temperature throughout practically all of the drying period. These data were sufficient for the calculation of the instantaneous drying rate and with the equilibrium moisture data permitted the calculation of the free moisture content.

One of the time-weight runs was made with a thermocouple imbedded in the center of the ramie slab to measure the temperature at the half-thickness of the slab. This copper-constantan thermocouple, made of fine wires, ran parallel to the surfaces of the slab, equidistant from each surface, from the edge of the slab to its geometric center. Connections were made to a Leeds-Northrup potentiometer and a cold reference junction of 32 $^{\circ}$F which were located outside of the dryer. Provisions were made for disconnecting the potentiometer and cold junction for weighing the slab. Readings of the thermocouple potentiometer were made just prior to each weighing while the slab remained in the dryer.

The air velocity across the surfaces of the slab were measured with two velocity tubes connected to a draft guage filled with ethyl alcohol. The tubes could easily be moved about so that the air velocity could be measured at any point in the drying compartment. The draft guage was inclined at a slope of 1:38. This made readings of a thousandth of an inch of alcohol or better possible. Assuming an error in reading the draft guage of a thousandth of an inch and an error of three hundredths in determining the tube factor, the air velocity can be determined with an error of 3.8% at 140°F, 1% relative humidity and 500 ft/min, and an error of 3.3% at 140°F, 1% relative humidity and 1000 ft/min. The error at higher temperatures and relative humidi-

ties is a little greater.

For each run the slab was allowed to remain in the dryer an hour or more after obtaining an apparent constant weight in order to determine if a constant weight had really been obtained. Two slabs were allowed to remain in the dryer twenty-four hours after obtaining an apparent constant weight. Further loss in weight amounted to two tenths of a gram which is a very small error for a forty-three gram sample. This is the weight used for all runs except in those where the dry density of the fiber was varied. This served as a check on how close the drying sample had approached equilibrium after obtaining an apparent constant weight at the end of each run.

THEORETICAL CONSIDERATIONS

Drying is the term generally used to indicate removal of water from a system or structure, when the amount of water present is comparatively small. By far the most important processes for drying solids depends upon first vaporizing the water and in this form separating it from the structure of which it formed a part. If air or some inert gas is used to carry away the water vapor formed, the process is called air drying (28). This is the method used in this study.

Dryer design involves two separate yet dependent considerations. First, the moisture must be brought to the surface of the material to be dried, or to some point in the material, and at this point evaporated. Second, the drying medium must be brought into contact with the stock under proper conditions. The first consideration is commonly associated with drying theory: while the second, although a function of the first, involves largely the principles of fluid and heat transfer. It is the former that is to be reviewed here.

It is a well established fact that when any material is exposed to a constant atmosphere there will be an interchange of moisture between the two until a final value is reached which is unchanged by by further exposure. This condition represents equilibrium between the material and the atmosphere; and the moisture present is known as the equilibrium moisture. The equilibrium moisture is dependent upon the temperature and relative humidity of the ambient atmosphere and upon the nature of the material. Experiments have also shown that it is dependent somewhat upon the history of the material (13)(29)(34). The importance of equilibrium moisture to drying considerations can be seen since it represents the degree to which a substance can be dried in a

given atmosphere.

By analogy with other physical phenomena it is logical that the rate of approach to equilibrium conditions would be a function of the displacement from equilibrium. This leads to the distinction of the free moisture content or the total moisture present minus the equilibrium moisture. The equilibrium moisture is sometimes referred to as the bound moisture. The free moisture is the amount of water that can ultimately be removed by the given drying conditions.

If, when the material to be dried is first exposed to the drying atmosphere, the surface is completely wet with water, the drying process is similiar to the evaporation of water from a free liquid surface (1)(28). As long as the surface remains wholly wet, the rate of evaporation is not a function of the water content of the material; and under constant drying conditions the rate of drying is constant. This period is called the "Constant Rate" period. After reaching a certain moisture content the drying rate begins to decrease, and the so-called "Falling Rate" period begins. The moisture content at which the change from a constant to a falling rate occurs is known as the critical moisture content.

Experimental evidence indicates that during the constant rate period liquid moisture is moving to the surface of the solid at a rate equal to that of the evaporation from the surface (1)(3)(8)(10)(11)(13)(14)(15)(16)(21)(22)(28)(34). If the drying occurs adiabatically, the equilibrium temperature reached by the solid approaches the wet bulb temperature of the drying air. When heat is supplied directly to the stock by conduction from adjoining dry surfaces or by radiation from the surroundings, then the surface temperature is higher than the wet

bulb temperature, and the drying rate is increased. An initial adjustment period usually exists during which the wet material comes to the equilibrium temperature which is to prevail during the constant rate period.

During the constant rate period the rate of drying as weight of water per unit time removed from a wet surface of a given area may be expressed to good agreement by the equation (1)(22)(28):

$$dW/d\theta = K_g A(H_s - H_a) \tag{1.01}$$

or for a unit area as

$$dW/d\theta = K_g(H_s - H_a) = K_g(\Delta H). \tag{1.02}$$

The constant K_g is the film coefficient and is a function of the air velocity, angle of incidence of the air to the solid, temperature, and other variables that affect the film resistance to heat and mass transfer. For most purposes K_g can be expressed as a function of air velocity over relatively short ranges of temperature by the equation (1)(28)

$$K_g = \propto G^n. \tag{1.03}$$

Substituting equation (1.03) into (1.02) gives:

$$dW/d\theta = \propto G^n(\Delta H). \tag{1.04}$$

The nature of the drying mechanism during the falling rate period is not as definite not is as thoroughly understood as for the constant rate period. For a good many substances, i.e., wood, certain clays and brick mixes, unglazed ceramic products, soaps, etc., the

process is divisible into two secondary periods, which from the mechanisms of drying prevailing in each may be called the "zone of unsaturated surface drying" and the "zone where internal liquid diffusion controls" (23). The former period follows immediately after the critical point; the decrease in the rate of drying in this zone is due to the decrease in the wetted surface of the material. The mechanism of the drying is essentially the same as for the constant rate period; but dry portions of the solid protrude into the air film so that the rate of evaporation per unit of total surface is reduced.

The maximum rate of diffusion of water to the surface decreases with the water content of the material (21)(22)(28). This causes a second critical point to be reached beyond which the resistance to internal liquid diffusion is greater than the surface resistance to vapor removal. During this period the rate of internal liquid diffusion controls the rate of drying. Also during this period air velocity has no influence on the rate of drying; and air humidity is of importance only so far as it affects the equilibrium moisture content.

Diffusion equations have been solved for certain limits and applied to data during this period of diffusion controlling with a great deal of success by a number of investigators (10)(13)(17)(18) (21)(23)(24). It should be pointed out, however, that there is still controversy as to just what materials the diffusion equations may be applied without experimental data (11)(15)(27).

For a number of other substances, notably fibrous materials, certain sands and clays, and brick mixes, the mechanism during the falling rate period is not as clearly understood, nor can data for

these substances be correlated as well. One thing is definite; the data does not follow the diffusion equations, nor does it follow simple relationships developed upon the assumption that the drying rate in the falling rate period is a linear function of the free water present under constant drying conditions.

Knowing full well his simplifying assumptions, Lewis developed the following equation for drying during the falling rate period (13) (28):

$$-\frac{dT}{T-E} = \frac{d\theta}{L(r_i + r_s)} = Ed\theta \tag{1.05}$$

where

$$r_i = L/3D \tag{1.06}$$

and

$$r_s = \rho(T_{sc} - E)/\theta \quad . \tag{1.07}$$

His assumptions were:

1. That the constant rate period was long enough for a parabolic concentration gradient to be established in the slab, and that it remain parabolic during the falling rate period.

2. That the diffusion law holds. That the driving force for diffusion of moisture is the concentration gradient in the material.

3. That the instantaneous rate of evaporation per unit surface is proportional to the difference between the surface concentration and the concentration corresponding to equilibrium with the main body of air flowing past the surface.

It is seen that B is a function of thickness, temperature, humidity, and the angle of incidence of the air stream.

Upon neglecting shrinkage and assuming r_i and r_s constant, integration between limits of $\theta = 0$ and $T = T_1$ and θ and T, gives:

$$\ln\frac{T_1 - E}{T - E} = \frac{\theta}{L(r_i + r_s)} = B\theta \tag{1.08}$$

Where both resistances are important, eliminating r_i and r_s from equation (1.08) gives:

$$\frac{1}{B} = \frac{\theta}{\ln\frac{T_1 - E}{T - E}} = L\left[\frac{L}{3D} + \frac{\rho d(T_{sc} - E)}{\theta}\right] \tag{1.09}$$

If resistance to surface evaporation is controlling:

$$\ln\frac{T_1 - E}{T - E} = \frac{\theta}{r_s L} = B\theta \tag{1.10}$$

If resistance to liquid diffusion is controlling:

$$\ln\frac{T_1 - E}{T - E} = \frac{3D\theta}{L^2} = B\theta \tag{1.11}$$

Since these relationships are derived on the assumption that the diffusion law holds for the movement of water to the surface of the material being dried, they should not necessarily be good for analyzing drying rate data of materials where the moisture does not move by diffusion. However, it has been found that they agree to fairly good approximation with heelboard (13), whiting (28), and rayon (30). This does not mean, however, that the mechanism of drying of these substances is by the movement of water to the surface by liquid diffusion. These relationships have proved useful in approximating

drying rate curves for these substances at conditions other than those used in the experimental work.

For convenience equation (1.08) may be simplified by substituting for B

$$B = \alpha G^n (\Delta H) \tag{1.12}$$

and thus obtaining

$$\ln \frac{T_1 - E}{T - E} = \alpha G^n (\Delta H) \theta \tag{1.13}$$

This relationship has been found to be very good for the drying of rayon (30).

For the entire falling rate period the drying rate can be expressed as a function of the free moisture content for any substance so far investigated. however, just what this relationship is has never been thoroughly understood or developed for fibrous and granular materials from a theoretical standpoint, where the movement of water to the surface of the material is not controlled by moisture concentration gradients. Indeed, the movement of liquid moisture through fibrous and granular materials is controlled mainly by capillary and gravitational forces (4)(15)(27). It has been demonstrated that it is possible for moisture to move from higher moisture concentrations to lower moisture concentrations by capillary forces. This is because forces causing movement by capillary action are a function of the diameter of the capillaries for a given liquid and not of the moisture concentrations in the material. This the the exact opposite of the conception of the movement of liquid water through a material by the process of diffusion.

One of the most thorough of the investigations of capillary flow[2] was carried out by Ceaglske and Kiesling (4). They found that capillary flow could be expressed by a modified form of Darcy's Law:

$$v_x = -\frac{k}{\rho} \frac{dP}{dx} \tag{1.14}$$

where P is the capillary potential or suction and is defined as the pressure difference between the water and the air at the curved air-water interface, the curvature being produced by the surface tension of the water. For vertical flow equation (1.14) must be modified to take in effects of gravity:

$$v_x = -\frac{k}{\rho} \frac{d(P - (-\rho x))}{dx} \tag{1.15}$$

where $(-\rho x)$ is the gravity potential. They obtained data which showed that capillary forces are equally as effective in producing flow as are external forces in saturated flow. They also demonstrated that of the two forces causing flow of moisture in a material containing capillaries, capillary suction and the moisture concentration differences, capillary suction is the factor causing flow. The moisture concentration depends upon the total suction and is not the prime factor in causing flow. The diffusion of vapor from surfaces with large radii to surfaces with small radii of curvature can be neglected because this diffusion process is extremely slow.

They further discovered that equations (1.14) and (1.15) only

---

[2]Capillary flow is defined as the type of flow existing when a liquid is flowing through a porous media without assistance of an external force.

apply until the suction reaches the entry suction value. Entry suction is that value of suction necessary to cause a sudden drop in the moisture content with no appreciable increase in the total suction. It is reasonable to expect the permeability (k) to drop after the entry value is reached since air is now entering the pores which in turn decreases the cross sectional area available for flow. Permeability of course is a function of the temperature, the fluid and the material.

The total suction may be made greater than the entry suction by either of two methods. First the total column height may be greater numerically than the entry suction. The layer of material which lies above the entry value would have a very low permeability and the rate of flow possible from such a column would be very small. Furthermore any flow would increase the total suction at the surface resulting in a decrease in the permeability. With a column sufficiently high the permeability becomes essentially zero, so capillary flow up the column is impossible. Now if the column is not as high numerically as the entry suction, then any flow will increase the total suction. Continuing the increase in flow will eventually cause the total suction to reach the entry value and further increase in flow will be impossible because of the rapid decrease in the permeability. The maximum flow possible decreases rapidly as the column height approaches the entry value.

In either of the cases discussed above the actual column height need not be the height given. Consider a column twenty-five cms. high under equilibrium conditions. If the bottom twenty cms. of this column are removed the conditions in the top five will not be altered.

The effective height used to determine the permeability of the top layer would be twenty-five cms. even though the column was only five cms. high. The bottom of the five cms. layer would have an equilibrium suction of twenty cms. and the top twenty-five cms. Obviously since there is no supply of water at the bottom of this short column the flow would now be unsteady state flow if there were any flow at all.

Although the investigations by Ceaglske and Kiesling were carried out on very fine sands, it is reasonable to assume that the same forces are at work in fibrous materials where spaces between fibers leave a complete maze of capillaries.

Another interesting phenomenon is the vapor pressure lowering of water in very fine capillaries (3). For example a capillary with a radius of a thousandth of a micron will lower the vapor pressure of water in it fifty percent below normal while a capillary with a radius of one micron will lower the vapor pressure of water only eleven hundredths of one percent (3).

Recent electron microscopal studies of ramie show that the smallest filaments visible with the naked eye are composed of even smaller "fibrils" with plenty of fine capillaries between the fibrils. They further show that the fibrils are in turn composed of even finer fibrils which seem to be the basic structural element of ramie (12). These smallest fibrils average three hundred sixty Angstrom units in diameter and it is believed, although not proven, that they are com-posed of chains of cellulose molecules. Therefore, the structure of ramie may be visualized as a complete maze of entwining and inter-linking capillaries of a wide range of diameters, many of which are well below one micron. From these studies one would assume that the

moisture flows mainly by capillary action in a drying process.

Although ramie fiber has an absolute density of better than 1.5 gm/cc (9), it is very difficult to pack it to apparent densities of greater than 0.300 gm/cc without the aid of mechanical presses. Thus the space occupied by the capillaries is relatively large compared to the space occupied by the "solid" fibrils of ramie.

PRESENTATION AND ANALYSIS OF RESULTS

The equilibrium moisture data for the fiber is given in Fig. 4 along with Reid's data (34). The data obtained agreed with that reported by Reid within experimental error. The general shape of the curves is similiar to those found in the literature for other textiles (13)(28)(29)(30)(31)(32).

Drying rate curves with all variables held constant except air velocity are shown in Fig. 5. The erratic behavior of the curves is due to non-uniform moisture distribution in the slabs at the beginning of the run because of air bubbles and pockets. These occured in the slabs of fiber if they were not squeezed and beaten during the soaking process. No shrinkage was noted during these or any later runs. At high densities there was some tendency for the slab to expand slightly as it dried out. This was probably due to the release of capillary suction which kept the slab more compact while wet. However the expansion just was enough to be noticeable.

The curves shown in Fig. 6 are for the run where a thermocouple was imbedded in the geometric center of the slab in order to measure the temperature there during drying. The drying rate curve exhibits a typical constant rate period followed by a falling rate period. This was found to be true for all drying rate curves obtained in this study. It is seen that the temperature at the center of the slab remained constant at the wet bulb temperature until the percent free moisture dropped to about fifteen percent, at which time the vaporization zone or at least a portion of it reached the center of the slab.

The overall heat transfer coefficient from the ambient air to the

slab center was computed by the equation

$$U = \lambda S/(t_a - t_z) , \qquad (1.16)$$

assuming that all heat was utilized in evaporating the water in the slab and that none was used in heating up the dried portion of the fiber. This assumption is justifiable as the latent heat required to evaporate a gram of water is several hundred times the heat required to raise the temperature of a gram of ramie a few degrees.

The overall coefficient, U, remained constant during the constant rate period indicating evaporation at the surface. During the falling rate period, however, it decreased, indicating that the limit of at least a part of the zone of vaporization was retreating gradually into the slab[3]. At a free moisture content of about fifteen percent, U became essentially constant indicating the zone of vaporization or portions of it reached the center of the slab. This also is the point at which the temperature at the center of the slab began to rise. A slight bend in the drying rate curve is noted at the same free moisture content producing a "bump" between zero and fifteen percent free moisture content. This can be attributed to the fact that at this point the vapor pressure in the slab was no longer a function of the temperature of the free water in the slab, i.e., the wet bulb temperature of the air, but depended upon the temperature and the highest bound water concentration still remaining in the slab. The bound water present in the center of the slab at this point is in all probability greater than the bound water at the surface of the slab.

_____

[3] U remains constant under similar conditions for wood and parchment where diffusion is the controlling factor in drying (15)(28).

This may be explained by the fact that the water vapor diffusing
through the pores of the slab from the zone of vaporization to the
surface of the slab, form an atmosphere within the pores of the slab
of a higher humidity than that of the drying atmosphere. This higher
humidity causes a higher equilibrium moisture or bound moisture con-
tent within the slab than at the surface. The rise in temperature in-
creases the rate of diffusion of the vapor to the surface of the slab
and at the same time decreases the equilibrium moisture content at
points within the slab, making more water available for evaporation.
Thus the rise in the drying rate at this point above the trend expect-
ed.

In Fig. 7 may be seen five drying rate curves of different air
velocities with all other variables held constant. All exhibit typi-
cal constant rate and falling rate curves of similiar shape. The cri-
tical moisture content increases with increasing air velocity which is
typical for most substances that have been investigated. The outstand-
ing feature of the curves is the change in drying rate with change in
air velocity at all free moisture concentrations[4]. If diffusion were
an important factor in the drying mechanism at any time during the
falling rate period, this phenomena would not be possible. Apparently
certain capillaries or a connection of capillaries in the fiber has
access or connections to areas of moisture in the slab that feed water
up to the surface of the slab until the free moisture content is near
zero. Or expressed in another way, the entry suction is not reached
for certain capillaries with openings on the surface until the free

_____

[4] Reid reported this phenomena, but inasmuch as his technique of
measuring air velocity was not good, the proof was not definite (34).

moisture concentration for the entire slab in very near zero. That the surface terminus of these capillaries is not a major fraction of the total area of the surface is seen from Fig. 6 where the decrease in U indicates a retreatment of the larger portion of the zone of vaporization into the slab. The changes in the slope of the curves during the falling rate period cannot be explained precisely without a thorough knowledge of how much of the zone of vaporization retreats into the slab at a given time and how far, and without a relationship based upon theoretical considerations of the forces involved that fit the data. Its gradual change of slope does, however, show that there are no "critical points" within the falling rate period where a large portion of the zone of vaporization either begins retreating below the slab surface or retreats suddenly at a greater or lesser rate.

The effect of variation of humidity, both absolute and relative, is shown in Fig. 8. Here the effect is the same as for most substances in the constant rate period, and is proportional to the change in humidity gradient across the film. This proportionality continues throughout the entire drying process. In general the percent free moisture at the critical point decreases with increasing humidity. This has been found to be true of most substances.

Shown in Fig. 9 is the variation of drying rates with temperature at a constant relative humidity. The absolute humidity changed with the temperature, so the change in rates shown really are for variation of temperature and absolute humidity. Increasing temperatures at constant relative humidities increases ΔH thus increasing the drying rates. Slight charring of fine fibers near the surface occurred at temperatures of 170 $^\circ$F and 200 $^\circ$F. Therefore, temperatures in this

range should not be used commercially where fiber color and physical appearance are important. No charring occurred at all at 140 °F.

The influence of slab thickness on drying rates is shown in Fig. 10. The results agree well with those reported for paper pulp (15). It is seen that for a given free moisture concentration in the falling rate period, the thicker the sample, the slower the drying rate. This can be explained in the following manner. Consider the conditions in two slabs of different thickness that are drying at the same rate during the falling rate period, but before all the free moisture has been removed. If the rate of water loss is the same in the two slabs, the condition of the zone of vaporization in each will be identical in all respects. The zone of vaporization in the thin slab will be a larger fraction of the total slab than that in the thicker slab. Thus the average water concentration in the thicker slab will be greater than in the thinner one. This causes the change in the drying rate curves in the falling rate period from concave down for thin slabs to concave up for thick slabs.

Figs. 11 and 12 show the change in drying rate with change in the dry density of the fiber, all other variables being held constant. Note that increasing density shifts the critical moisture content to the right. The drying rate in the falling rate period is very much the same for small density changes, but decreases for equal free moisture content when the dry density is doubled. This means of course that the critical moisture content cannot be expressed on a volume basis for a given drying rate in the constant rate period at varying dry densities. Indeed, the moisture content of the denser slab is greater at the critical point than for the less dense slab,

despite the greater void space in the less dense slab. Evidently the denser slab provides shorter capillary connections to free water areas in the slab causing the entry suction to be reached more rapidly than for the less dense slab. Also the permeability of the denser slab is lesser due to a decrease in cross-sectional area available for movement. The decrease in drying rate in the falling rate period can be explained by the increase in resistance of diffusion of vapor from the retreating zone of vaporization to the surface. This resistance is increased due to less void space and smaller pore openings in the denser slab. It should be pointed out that this does not agree with the data obtained on two runs of paper pulp at different densities reported in the literature (15). However, only two runs were presented and they were made at different thicknesses as well as different densities. Therefore, it is difficult to draw any positive conclusions from them.

If the logarithm of the drying rate in the constant rate period by plotted against the logarithm of the mass velocity of the air, the slope of the line thus obtained should be equal to the exponent n of equation (1.04), provided all other variables are held constant. This has been done in Fig. 13 for those runs plotted in Fig. 7. The exponent thus determined has a value of 0.84 which agrees well with values reported in the literature not only for drying, but for heat transfer as well (1)(28).

In Fig. 14 is plotted drying rate in the constant rate period versus ΔH. For those runs where ΔH was changed by changing the relative humidity at constant temperature a good straight line is obtained indicating that the drying rate is a direct function of ΔH. It can also be seen that a reasonable straight line can be drawn

through the points representing runs where $\triangle H$ was changed by a change in temperature at constant relative humidity. The slope of the two lines is not the same indicating that $\propto$ in equation (1.04) is a function of temperature. This is to be expected since temperature effects the film thickness and the rate of diffusion through it. The effect seems to be relatively small compared to the effect of air velocity on the film, however, and for relatively small temperature changes may be neglected. This point can be brought out more clearly by the computation of $\propto$ for the runs concerned. These values are tabulated below. The values of $\propto$ were computed using the following

Temperature, ^{o}F	$\propto$
140	0.872
170	0.799
200	0.765

units for terms in equation (1.04): G, lb/hr-ft^2; dW/dθ, gms/hr-cm^2; $\triangle H$, lb H$_2$O/ft^3 bone dry air. It is seen that $\propto$ decreases with increasing temperature but not linearly. Probably the increase in the rate of diffusion due to higher temperatures is offset by the increase in the thickness of the film due to increase in viscosity of the air with rising temperatures.

If the concentration of free moisture in gm/cc at the critical point be plotted against the drying rate at the critical point as in Fig. 15, a straight line can be drawn through those points for runs made at the same dry density. Those points made at a different dry density fall far from the straight line drawn. Thus the correlation of moisture concentration data on a volume basis at the critical point is good only for equal densities. For different densities a different correlation must be worked out. The cause of this phenomena has been

explained in the paragraph on change of drying rates with dry density.

Although the restrictions for equations (1.05) through (1.11) have been pointed out and the fact emphasized that there is no theoretical reason why they should apply to the drying of this type of material, since they have been applied with some success to other fibrous materials an attempt was made to apply them to ramie fiber. The plots are shown in Figs. 17-19. In Fig. 17 all variables were constant except air velocity. In Fig. 18 all variables were constant except relative humidity. In Fig. 19 thickness and temperature were varied while all other variables were held constant. Examination of the plots show that in most cases imagination has to be used in order to get a good straight line, and below a value of 0.1 for W/W_c the relationship fails altogether. Note that the free moisture content for a value of W/W_c of 0.1 is about fifteen percent. This corresponds to the "hump" on the drying rate curve in Fig. 6 as previously brought out. The deviation from a straight line for values of W/W_c greater than 0.1 seems to be smallest for high drying rates, but even so, the correlation is not exact. This is not surprising in view of the previous mechanism discussions. The fact that the movement of water by capillary forces coupled with vapor diffusion from the retreating zone of vaporization are similiar to movement by liquid diffusion alone is coincidence. However, this is the best simple relationship tried which fits the data obtained, and can be used for most approximations over the ranges it has been proven to hold.

Inasmuch as the data fit equations (1.05) through (1.11) approximately, values of B were calculated assuming a straight line could be drawn through the points in Figs. 17 through 19. Using the

simplified relationships (1.12) and (1.13) Fig. 16 was constructed. It can be seen from equation (1.12) that if the logarithm of B is plotted against the logarithm of mass velocity the slope will give the exponent n. The value of the exponent was determined to be 0.73 for slabs of ramie 1.27 cms. thick. This value has been reported in the literature as 0.5 for heelboard (13) and as 0.5 on up to values above one for rayon (30) depending on the condition of the rayon and the ratio of surface area to the dry weight of the rayon. The data on rayon was reported as the rate of drying per unit weight of stock, while the data on heelboard was reported as the rate of drying per unit area exposed to the drying atmosphere.

To further test the validity of equations (1.12) and (1.13), the values of $\propto$ were computed from equation (1.12) to see if it were constant at a temperature of 140 °F. The results are shown below. It is

Run No.	$\propto$
4	1.14
5	1.04
6	1.18
7	1.14
8	1.12
9	1.22
10	1.04
11	1.18
Ave.	1.12

seen that $\propto$ is fairly constant with changes in ΔH or G at a constant temperature, so that equation (1.12) is reasonable valid for ramie. The fact that a reasonable straight line can be drawn through the points in Fig. 16 further substantiates the fact. It must be remembered that all of these calculations were based on the assumption that a straight line could be drawn through the points plotted in Figs. 17 through 19.

Since the data does seem to fit the equation developed by Lewis with a fairly good degree of approximation, they should fit the case where both resistances to diffusion and surface evaporation are important controlling factors. It has already been shown that the resistance to surface evaporation is a controlling factor at all free moisture concentrations. The diffusion of the vapor from the zones of vaporization inside the slab to the surface, while not occurring throughout the entire slab is a controlling factor also. It can be seen from equation (1.09) that a plot $1/BL^2$ versus $(T_{sc}-E)/\beta L$ should give a straight line. Since $\beta = h(t - t_s)/\lambda$ and since E is a relatively small quantity for this material, $(T_{sc}-E)/\beta L$ is proportional to $(1/L)(t - t_{sc})$. Since t_{sc} closely approaches the wet bulb temperature of the air, these data are plotted in Fig. 20 as $1/BL^2$ versus $(1/L)(t - t_W)$. It is seen that a good straight line is obtained as called for except for two points. It is to be remembered that these same runs give poor values for T_{sc} on Fig. 8. It is to be remembered that the value of B used in making the plot of Fig. 20 was determined assuming that a straight line could be drawn through the points on Figs. 17 through 19. This is not quite true so this relationship is only another approximation that happens to work over the ranges investigated.

The agreement with Lewis's equations being fairly close it was decided to determine if it would fit equations (1.10) or (1.11) in order to get an idea as to whether the resistance to surface evaporation completely controls during the falling rate period. Examination of these equations show that if log θ be plotted against log L for equal values of $T_1 -E/T - E$, the slope should give the exponent

of L. For the case where surface evaporation is controlling the exponent is unity. For the case where internal diffusion is controlling the exponent is two. Fig. 21 shows the slope to be 1.16 which is the value of the exponent of L, assuming that a straight line can be drawn through the points plotted in Figs. 17 through 19. This would indicate that even provided Lewis's equations could be applied to ramie fiber on a theoretical basis, surface evaporation would not be the controlling factor. Therefore, if these equations are used in attempts to approximate drying curves for ramie, equation (1.09) is the best one to use. Equations (1.10) and(1.11) cannot be used in an attempt to simplify equation (1.09) without introducing further error. It should be remembered that these relationships if used are only good approximations for the ranges so far investigated. These ranges should cover most conditions met in drying practice.

Summing up, the data and analysis presented indicates the mechanism of drying of garnetted ramie fiber to be as follows. In the constant rate period water moves up to the surface of the fiber by capillary action, and is there removed by evaporation at a rate determined by air velocity and other factors influencing the film characteristics. As soon as the entry suction is obtained at certain points on the surface, the surface film of water is broken, the critical point is passed and the falling rate period begins. Ceaglske and Hougen have shown experimentally that the critical point occurs at the same free moisture content at which the entry suction value is reached (3). The drying rate continues to decrease due to three principal factors. More and more portions of the surface reaches the entry suction causing the vaporization zone to retreat into the fiber at more points. Those vaporization zones already inside the fiber retreat further from the

surface, increasing the distance to be traversed by the diffusion of
vapor to the surface. This also increases the distance heat must
traverse to the free moisture or the zone of vaporization. The
vaporization of the water from the zones of vaporization within the
slab is less due to the small radii of curvature. Water is evaporated
at the slab surface at the terminals of certain capillaries whose
entry suction is never reached throughout the entire drying process.
The number of such capillaries continually decreases from the time
the critical point is reached until zero free moisture is obtained.
This mechanism continues until the free moisture content drops to
about fifteen percent at which time a rise in temperature within
the slab increases the diffusion of vaporized water to the surface
of the slab and decreases the bound or equilibrium moisture to its
value corresponding to the surrounding atmosphere.

It is realized that ramie fiber will probably never be dried
commercially in the form of slabs. This was merely an experimental
technique used to study the mechanism and characteristics of drying.
However, these same mechanisms and characteristics occur in the drying
of ramie fiber, no matter what it physical shape.

It is hoped that this work has shed some light on an under-
standing of the mechanisms involved in drying ramie fiber and fibers in
general, and that this knowledge can be used in developing and improv-
ing equipment and drying processes for ramie and other fibers.

NOMENCLATURE

A   Area, cm^2

B   A constant

D   Diffusivity of liquid

E   Weight of equilibrium moisture, gms.

h   Coefficient of heat transfer from air to surface

       of fiber

H_s Absolute humidity, wt. H_2O per unit wt. bone dry air corresponding to saturation at surface temperature

H_a Absolute humidity of the drying atmosphere

ΔH $H_s - H_a$

K_g Film coefficient for diffusion through film

k   permeability

L   Half thickness of slab, cm.

P   Capillary potential or suction in cms. of fluid height

r_i Resistance to internal diffusion

r_s Resistance to surface evaporation

S   Surface evaporation, $gm/hr-cm^2$

t   Temperature of air ^oF

t_a Temperature of air ^oC

t_s Temperature at surface ^oF

t_{sc} Temperature at surface at critical point ^oF

t_w Wet bulb temperature of air ^oF

t_z Temperature at center of slab ^oC

T   Total weight moisture, both free and bound, gms.

T_{sc} Total wt. water at critical value

U   Overall heat transfer coefficient, $cal/hr-cm^2{}^oC$

v_x Velocity in direction x

W   T - E, weight free moisture, gms.

θ Time, hours

Greek Letters

$\propto$ Constant

β $h (t - t_s)/\lambda$

λ Latent heat of vaporization

ρ Density of liquid, gm/cc

ρ_D Dry density of fiber, gm/cc

FIG 7
CALIBRATION OF VELOCITY
TUBES
RELATIVE HUMIDITY 19%

FIG 2
CALIBRATION OF VELOCITY TUBES
TEMPERATURE   140°F

FIG. 3
CALIBRATION OF THERMOCOUPLE
REFERENCE JUNCTION 32°F.

40

FIG. 4. EQUILIBRIUM MOISTURE CONTENT OF DEGUMMED OPENED RAMIE

REIDS DATA   HANCOCKS DATA
DESORPTION   x
+   ABSORPTION   □

DRYING RATE - GMS/HR-CM²

PERCENT FREE MOISTURE

0.0   40   80   120   160   200   240   280   320   360

VARIATION OF DRYING RATES
CAUSED BY DIE-CASTERS FOR
MAXIMUM OVENT MOISTURE 19%
THROUGHOUT

TEMP DB 140 WB 95-4
REL HUM 19%
THICKNESS 35   12 CM
DRY DENSITY 0130 4Kc
AIR VELOCITY

1		329 LB/FT²-HR
2	473	
3	568	

FIG. 6
HEAT TRANSFER DURING DRYING OF
CIGARETTE RADIO PAPER AT CONSTANT
START DRYING CONDITIONS

FIG. 6 DATA

TEMP	250-260	WB 150
REL. HUM.		79 %
AIR VELOCITY		4.73 LB/HR FT
		0.530 GM/CC
THICKNESS		127 CM
RUN. NO.		

DRYING RATE
TEMP. AT CENTER
OF SLAB
U- OVERALL HEAT
TRANSFER COEFF.

FIG. 7. DATA

TEMP. DB. 140 ± 2.95°F
REL. HUMIDITY 1.9%
THICKNESS 1.27 CM
DRY DENSITY 0.1280 G/CC
AIR VELOCITY (G) 1317 LB/F²-HR

AAF (KARASTIN?) DRYING WITH ... HUMIDITY
FIG. 9 DATA

THICKNESS	1.27 CM	
DRY DENSITY	0.130 GM/CC	
AIR VELOCITY	413 LB/FT/HR	

RUN NO.	DB	WB	RH
9	140	118?	51
10	140	108	38
11	140	100	25
6	140	95	19

DRYING RATE - GMS/HR-CM²

PERCENT FREE MOISTURE

DRYING RATE - GMS/HR-CM²

PERCENT TRUE MOISTURE

RATE VELOCITY WITH TEMP			
FIG 9 DATA			
THICKNESS 1.21 CM			
DRY DENSITY 0.730 GM/CC			
AIR VELOCITY 47.5 1.60? FT-HR			
RUN N°	D-B	W-B	R-H
8	6 140	95	19
"	12 170	115	19
"	13 200	135	19

FIG. 19
DATA VARIATION WITH THICKNESS

TEMP. DB 140 WB 95
AIR VELOCITY 275 FT/MIN
REL. HUM 19%
DRY DENSITY 0.730 GM/CC

RUN Nº	THICKNESS
+ 14	2.54 CM
▲ 5	1.27
● 15	0.64

DRYING RATE — GMS/HR-CM²

PERCENT FREE MOISTURE

MAX SATURATION WATER DENSITY

FIG. II DATA

TEMP 22°C N3700
RELATIVE HUMIDITY 75
AIR VELOCITY 47.5 CM/SEC
THICKNESS 1.27 CM
RUN NO   DRY DENSITY
o   74   0.611 G/CC
•   76   1.0161
*   77   1.520

DRYING RATE — GMS/HR-CM²

0.6
0.5
0.4
0.3
0.2
0.1
0.0

0   40   80   120   160   200   240   280   320   360
PERCENT FREE MOISTURE

RATE VARIATION WITH DENSITY
FIG. 72 DATA
TEMP. D.B. 140 W.B. 99
RELATIVE HUMIDITY - 73
AIR VELOCITY 4.2 FT/SEC
THICKNESS 1.17 CM

RUN NO.	DRY DENSITY
18	0.141 GM/CC
6	.0130
19	.0221

DRYING RATE — GMS/HR-CM²

PERCENT FREE MOISTURE

FIG.13
CORRELATION OF DATA DURING
CONSTANT RATE PERIOD.

FIG 13 DATA
CONSTANT RATE ANALYSIS
SLOPE = 0.84

DRYING RATE — GMS/HR·CM²

G - MASS VELOCITY · LBS/HR·FT²

50

CORRELATION FIG 1# DATA DURING
CONSTANT RATE DRYING PERIOD

FIG 1# DATA

AIR VELOCITY   472 LB/HR FT²
DRY DENSITY   0.130 GM/CC
THICKNESS   1.27 CM

RUN NO			
PT.1	9	7.40	.745	97
2	10	7.40	.745	88
3	11	7.50	.105	70
4	17	7.50	.105	45
5	6	7.40	95	29
6	12	7.70	.115	19
7	13	7.99	.135	13

DRYING RATE — GMS/HR CM²

B.H   LB H₂O VAPOR/LB BONE DRY AIR

51

FIG. 15
CORRELATION OF DATA AT
CRITICAL POINT

FIG 15 DATA
NOS. REFER TO RUN NOS.
RUNS 4 THROUGH 15
HAVE A DRY DENSITY
OF 0.130 GM/XC

FIG. 16
CORRELATION OF
DATA DURING THE
FALLING RATE
PERIOD.

FIG. 16
SLOPE   0.73

$G - LBS/HR - FT^2$

FIG. 17
CORRELATION OF DATA DURING THE FALLING RATE PERIOD.

FIG. 17 DATA

DRY DENSITY 0.130 G/CC
TEMP WB 140 DB 95
RH 19
THICKNESS 1.27 CM

RUN NO.	AIR VEL.	B
4	29.7 LB/FT²HR	1.71
5	37.9	1.93
6	47.3	2.48
7	56.8	2.79
8	66.3	3.07

TIME IN MINS.

FIG. 18
CORRELATION OF DATA DURING THE
FALLING RATE PERIOD.

FIG 18 DATA
DRY DENSITY   0.130 G/CC
THICKNESS   1.27 CM
AIR VELOCITY 473 LB/HR-FT²

RUN NO.	D.B.	W.B.	R.H.	B
o 9	140	118	51	1.59
▲ 10	140	104	30	1.86
• 11	140	100	25	2.26
□ 6	140	95	19	2.48

TIME IN MINS

FIG. 19
CORRELATION OF DATA DURING THE
FALLING RATE PERIOD

FIG 19 DATA

	AIR VELOCITY				
	DRY DENSITY				
RUN NO	D.B.	W.B.	R.H.	THICKNESS	B
12	170	115	19	1.27	2.94
13	200	135	19	1.27	3.45
14	140	95	19	2.54	1.02
15	140	95	19	0.635	5.35

TIME IN MINS.

FIG. 20
CORRELATION OF DATA DURING THE
FALLING RATE PERIOD

FIG. 20 DATA
DRY DENSITY - 0.130 G/CC

RUN NO.	D.B.	W.B.	R.H.	THICKNESS
8	140	95 F	19 %	1.27 CM
9	140	118	51	1.27
10	140	104	30	1.27
11	140	100	25	1.27
12	170	115	19	1.27
13	200	133	19	1.27
14	140	95	19	2.54
15	140	95	19	0.635

$1/B t^2$

$(t - t_w)/L$

0.01   0.02   0.03   0.04   0.05   0.06   0.07

FIG. 21
CORRELATION OF DATA
DURING THE FALLING
RATE PERIOD.

FIG. 21
SLOPE· 1/6

TIME IN MINS

THICKNESS IN CM.

BIBLIOGRAPHY

(1) Badger, W.L., W. L. McCabe, Elements of Chemical Engineering. New York: McGraw Hill Book Company, Inc., 1936 pp. 280-321.

(2) Bray, Helen A., Textile Fibers, Yarns and Fabrics. New York: D. Appleton and Company, Inc., 35pp.

(3) Ceaglske, N. H., O. A. Hougen, "Drying Granular Solids", Journal of Industrial and Engineering Chemistry, 13: 805-813, 1937.

(4) Ceaglske, N. H., F. C. Kiesling, "Capillary Flow in Porous Solids," Transactions of the American Institute of Chemical Engineers, 36: 211-225, 1940.

(5) Dodge, C. R., The Encyclopedia Americania. Vol. 23, 202 pp.

(6) Gilliland, E. R., "Fundamentals of Drying and Air Conditioning," Journal of Industrial and Engineering Chemistry, 30: 510-513, 1938.

(7) Glauert, H., The Elements of Aerofoil and Airscrew Theory, Cambridge: University Press, 1926. 483 pp.

(8) Hadlock, C., R. C. Brewer, C. B. Shepherd, "Drying Materials in Trays," Journal of Industrial and Engineering Chemistry, 30: 388-397, 1938.

(9) Hermans, P. H., D. Vermaas, "Density of Cellulose Fibers," Journal of Polymer Science, 1: 149-171, 1946.

(10) Hougen, O. A., "Rate of Drying of Chrome Leather," Journal of Industrial and Engineering Chemistry, 26: 333-339, 1934.

(11) Hougen, O. A., H. J. McCauley, W. R. Marshall, "Limitations of Diffusion in Drying," Transactions of the American Institute of Chemical Engineers, 36: 183-209, 1940.

(12) Kinsinger, W. G., C. W. Hock, "Electron Microscopical Studies of Natural Cellulose Fibers," Journal of Industrial and Engineering Chemistry, 40: 1711-1716, 1948.

(13) Lewis, W. K., "Rate of Drying of Solid Materials," Journal of Industrial and Engineering Chemistry, 13: 427-432, 1921.

(14) Lewis, W. K., W. H. McAdams, "Drying of Paper Pulp", Paper Pulp Magazine (Canada), 25: 122-129, 1927.

(15) McCready, D. W., W. L. McCabe, "The Adiabatic Drying of Hygroscopic Solids," Transactions of the American Institute of Chemical Engineers, 29: 131-159, 1933.

(16) Marshall, W. R., O. A. Hougen, "Drying Solids by Through Circulation," Transactions of the American Institute of Chemical Engineers, 38: 91-121, 1942.

(17) Newman, A. B., "Drying of Porous Solids: Diffusion and Surface Emission," Transactions of the American Institute of Chemical Engineers, 27: 203-211, 1931.

(18) _____, "Drying of Porous Solids: Diffusion Calculations," Transactions of the American Institute of Chemical Engineers, 27: 310-333, 1931.

(19) Nieman, H., "Progress in Ramie Development," Rayon Textile Monthly, Vol. XXVII, No. 9, Sept 1946.

(20) Ott, E., editor, Cellulose Derivatives, High Polymers, Vol. V. New York: Interscience Publishers, Inc., 130 pp.

(21) Sherwood, T. K., "Drying of Solids," Journal of Industrial and Engineering Chemistry, 21: 12-16, 1929.

(22) _____, "Drying of Solids - II," Journal of Industrial and Engineering Chemistry, 21: 976-980, 1929.

(23) _____, "Drying of Solids - III, "Journal of Industrial and Engineering Chemistry, 22: 132-136, 1930.

(24) _____, "Drying of Solids - IV," Journal of Industrial and Engineering Chemistry, 24: 307-310, 1932.

(25) Sherwood, T. K., E. W. Comings, "Drying of Solids - V," Journal of Industrial and Engineering Chemistry, 25: 311-316, 1933.

(26) Sherwood, T. K., E. R. Gilliland, "Drying of Solids - VI," Journal of Industrial and Engineering Chemistry, 25: 1134-1137, 1933.

(27) Sherwood, T. K,, E. W. Comings, "Drying of Solids - VII," Journal of Industrial and Engineering Chemistry, 26: 1096-1098, 1934.

(28) Walker, W. H., W. K. Lewis, W. H. McAdams, E. R. Gilliland,
     Principles of Chemical Engineering. New York: McGraw-Hill
     Book Company, Inc., 1937. pp 640-683.

(29) Wilson, R. E., T. Fuwa, "Humidity Equilibrium of Various
     Common Substances," Journal of Industrial and Engineering
     Chemistry, 14: 913-918, 1922.

(30) Withrow, J. R., H. F. Simons, J. H. Koffolt, "The Drying of
     Rayon," Transactions of the American Institute of Chemical
     Engineers, 39: 133-171, 1943.

(31) Weigerink, J. G., Textile Research, 10: 334-357, 1940.

(32) Weigerink, J. G., Textile Research, 10: 493-510, 1940.

(33) Anon., "Drying Conference Discussion," Textile Research, 6:
     431-442, 1936.

(34) Reid, T. F., "Equilibrium Moisture and Drying Characteristics
     of Textile Fibers," Thesis in Chemical Engineering,
     Georgia Institute of Technology, 1948, 93 pp.

APPENDIX

PREPARATION OF FIBERS

Professor J. L. Taylor, of the Textile Engineering Department, processed and supplied all the fiber studied.

The degummed garnetted ramie was Floridian ramie that had been thoroughly degummed and washed. The samples were passed twice through the garnett card to open the fibers thoroughly. This opened ramie analyzed 76.91% alpha cellulose.

SAMPLE CALCULATIONS

Calculations required for measuring air velocity were as follows. The factor for the tubes as shown in Table I, which is the factor between the head of fluid flowing past a pitot tube as compared to the head of the same fluid flowing past the tubes, was utilized with the slope of the draft guage filled with ethyl alcohol to produce a formula for computing air velocity. This formula simplified down to the following:

$$u = 253.8 \sqrt{G\,V}$$

where u in the velocity of the air flowing past the tubes in ft/min, G is the draft guage reading with the scale furnished, and V is the specific volume of the air. The specific volume of the air at various temperatures and humidities were obtained from the literature[5].

The above formula was used to prepare Figs. 1 and 2. A sample calculation for G at 600 ft/min and at a relative humidity of 10% and a temperature of 140 °F is shown below.

$$G = \frac{(600 \text{ ft/min})^2}{(253.8)(15.51 \text{ ft}^3/\text{lb})} = 0.364$$

Equilibrium moisture calculations for sample 1A, run 1 E is shown below:

Wet weight (sample and tare at equilibrium)	97.2506 gms.
Dry weight (sample and tare bone dry)	97.1860 gms.
Weight water present at equilibrium	0.0646

[5] Walker, W. H., W. K. Lewis, W. H. McAdams, E. R. Gilland, *Principles of Chemical Engineering.* New York: McGraw-Hill Book Co., Inc. 1937. p 720.

Dry weight   97.1860 gms.
Tare weight   93.6097 gms.
Bone dry fiber in sample   3.5763 gms.

Equilibrium moisture $\quad = \dfrac{0.0646}{3.5763}$

$$= \quad .0181 \text{ gms./gm}$$

$$= \quad 1.81\% \text{ dry basis}$$

The instantaneous drying rate of the fiber was arrived at as follows. From the weight-time data of the runs values of the drying rate in gms/hr-cm^2 were tabulated for each increment of time. The increment used was four and a half minutes as readings were taken every five minutes and exactly thirty seconds were allowed for weighing. These incremental drying rate values were plotted as the ordinate against $\Sigma \Delta \theta$ as the abscissa. An example is given in Fig. 22.
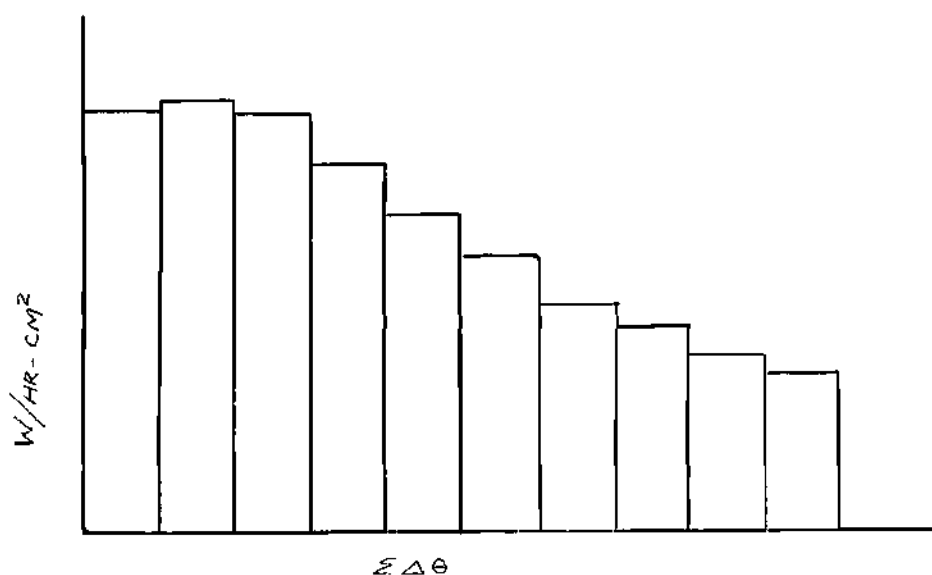
Plot of Incremental drying rates vs. time

Figure 22.

It is obvious that the area in each block is $\Delta W/cm^2$ or in all blocks W/cm^2. If $dW/d\theta$ had been plotted against $\leq d\theta$ or θ the area under the curve would also be W/cm^2. It follows, therefore, that if a smooth curve is drawn through the plot of the incremental drying rates versus $\leq \Delta\theta$ that at any time θ the smooth curve represents the instantaneous drying rate. It is evident that this is a method of approximation and is exact only in the limit as $\Delta\theta$ goes to zero. For the purpose of analyzing this data the method is sufficient.

To determine the free moisture content as a function of time it was assumed that when the drying sample had reached a constant total weight that equilibrium existed between the sample and the drying atmosphere. That this is not true has been shown by experiment[6]. However, in spite of the error involved the assumption is justifiable. The error has been shown to be very small.

Knowing the final total weight of the sample and the percent equilibrium moisture for the drying conditions, it is possible to calculate the weight of the dry sample. The difference between the total weight at any instant and the weight of dry fiber represents the amount of water present. Then the ratio of the weight of water to the weight of dry fiber is the total moisture content. The free moisture is this value of total moisture less the value of the equilibrium moisture.

For run 4 shown in Fig. 5, the final total weight of fiber equals 43.60 gms. and the equilibrium moisture is 2.0%.

$$\text{Bone dry fiber} = \frac{43.60}{1.020} = 42.75 \text{ gms.}$$

[6]Reid, T. F., "Equilibrium Moisture and Drying Characteristics of Textile Fibers," Thesis in Chemical Engineering, Georgia Institute of Technology, 1948, 93 pp.

At eighty minutes the total weight was 94.2 gms. ; 173.3 gms minus the weight of the suspension apparatus which was 79.1 gms. Therefore, the weight of water present was 51.45 gms. The total moisture content at this time was 1.203 lb/lb or 120.3% minus 2.00% equals 118.3% which is rounded off to 118%. This calculation was made for each recording of time-weight data.

The ratio W/W_c was computed by first locating the percentage free moisture from Figs. 6 through 12. The total weight of water was then determined by interpolation of time-weight data. From this the equilibrium water was subtracted to obtain the free water at the critical point. Then the weight ratio was determined at any time in the falling rate period with reference to the critical point.

For run 4 the critical point occurred at 114% free moisture. The total moisture at this point was determined by interpolation to be 47.55 gms. The equilibrium moisture was 43.60 minus 42.75 gms. equals 0.85 gms. (See above for figures.) Therefore the free moisture at the critical point was 47.55 minus 0.85 equals 46.70 gms. At 42.8 minutes past the critical point the total moisture was 15.25 gms. and the free moisture 14.40 gms. Therefore W/W_c at the time was found to be

$$= \frac{14.40}{46.70} = 0.308 .$$

This calculation was made for each point on Figs. 17 through 19.

A sample computation of U for Fig. 6 at 110 mins. is shown below.

$$U = \frac{(563 \text{ cal/gm})(0.183 \text{ gm/hr-cm}^2)}{(60°C - 35°C)} = 4.12$$

The values of $\propto$ for the constant rate period were calculated by use of equation (1.04). The computation for $\propto$ at a temperature of 170 $^{\circ}$F for run 12 is shown below.

$$\propto = \frac{0.44 \text{ gm/hr-cm}^2}{(47.3 \text{ lb/hr-ft}^2)^{0.64}(0.17 \text{ lb } H_2O/\text{lb dry air})}$$

$$= 0.799$$

The values of B were determined by use of equation (1.08) and Figs. 17-19 at values of W/W_c of 0.1. The time was obtained graphically at the intersection of the straight line drawn through the points with the line representing a value of 0.1 for W/W_c. A sample computation is shown below.

$$B = \frac{\ln 10.0}{50 \text{ mins.}} (60 \text{ mins./hr}) = 2.75.$$

The values of $\propto$ for the falling rate period were calculated from equation (1.12). The calculation of $\propto$ for run 9 is shown below.

$$\propto = \frac{1.37}{(47.3 \text{ lb/hr-ft}^2)(0.0067 \text{ lb } H_2O/\text{lb dry air})}$$

$$= 1.22 .$$

TABLE I

Determination of factor for velocity tubes.

Calibrated with Whélan Guage.

Zero Reading Ins Alcohol	Pitot Reading Ins. Alcohol	ΔH_p	Tubes Reading Ins. Alcohol	ΔH_t	$\Delta H_t/\Delta H_p$
0.4490	0.4535	0.0045	0.4575	0.0105	2.33
0.4490	0.4575	0.0085	0.4665	0.0175	2.06
0.4490	0.4550	0.0060	0.4633	0.0143	2.38
0.4490	0.5020	0.0530	0.5515	0.1025	1.94
0.4508	0.4814	0.0306	0.5130	0.0622	2.03

Room Temperature 27 deg. C.

Average Value of $\Delta H_t/\Delta H_p$ is 2.15

ΔH_t equals 2.15 x ΔH_p

TABLE II

Run 1E, Equilibrium Studies

Dry Bulb 140   Wet Bulb 95   Relative Humidity 19%

Sample*	Wet Weight Gms.	Dry Weight Gms.	Tare Weight Gms.	Equilibrium H_2O Gms. H_2O/g fiber
1A	97.2506	97.1860	93.6097	0.0181
2A	101.8652	101.7665	97.0913	.0211
3D	97.5416	97.4404	92.9882	.0198
4D	96.2884	96.2049	91.9880	.0198

Run 2E, Equilibrium Studies

Dry Bulb 140   Wet Bulb 106   Relative Humidity 33%

Sample	Wet Weight Gms.	Dry Weight Gms.	Tare Weight Gms.	Equilibrium H_2O Gms H_2O/g fiber
1A	97.7159	97.6280	93.6102	.0219
2A	102.2300	102.1096	97.0920	.0240
3D	97.0532	96.9524	92.9763	.0253
4D	96.8692	96.7459	92.0205	.0261

Run 3E, Equilibrium Studies

Dry Bulb 140   Wet Bulb 118   Relative Humidity 51%

Sample	Wet Weight Gms.	Dry Weight Gms.	Tare Weight Gms.	Equilibrium H_2O Gms H_2O/g fiber
1A	98.6953	98.5194	93.7542	.0369
2A	101.0990	100.9750	97.1056	.0321
3D	97.3206	97.1782	92.8765	.0330
4D	97.0377	96.8748	92.6394	.0385

*   A - Adsorption
     D - Desorption

TABLE III

Run 4E, Equilibrium Studies

Dry Bulb 170   Wet Bulb 115   Relative Humidity 19%

Sample*	Wet Weight Gms.	Dry Weight Gms.	Tare Weight Gms.	Equilibrium H_2O Gms H_2O/g fiber
1A	98.2114	98.1565	93.6132	0.0121
2A	101.4325	101.3814	97.1242	.0120
3D	97.5904	97.5288	92.8544	.0132
4D	96.7662	96.7005	91.9741	.0139

Run 5E, Equilibrium Studies

Dry Bulb 170   Wet Bulb 144   Relative Humidity 51%

Sample	Wet Weight Gms.	Dry Weight Gms.	Tare Weight Gms.	Equilibrium H_2O Gms H_2O/g fiber
1A	98.4312	98.3120	93.5478	.0250
2A	101.8347	101.7206	97.1052	.0247
3D	96.8706	96.7631	92.7650	.0269
4D	96.7741	96.6431	91.9767	.0281

* A - Adsorption
  D - Desorption

TABLE IV

Run 6E, Equilibrium Studies

Dry Bulb 200   Wet Bulb 135   Relative Humidity 19%

Sample*	Wet Weight Gms.	Dry Weight Gms.	Tare Weight Gms.	Equilibrium H_2O Gms H_2O/g fiber
1A	98.0169	97.9925	93.4486	0.0050
2A	101.9006	101.8773	97.1162	.0049
3D	97.0170	96.9873	92.8552	.0072
4D	96.7873	96.7487	91.9876	.0081

Run 7E, Equilibrium Studies

Dry Bulb 200   Wet Bulb 172   Relative Humidity 51%

Sample	Wet Weight Gms.	Dry Weight Gms.	Tare Weight Gms.	Equilibrium H_2O Gms H_2O/g fiber
1A	99.6595	97.5848	93.4585	.0181
2A	101.5363	101.4549	97.1273	.0188
3D	97.7363	97.6638	92.8954	.0152
4D	96.7207	96.6236	91.9762	.0209

* A - Adsorption
  D - Desorption

TABLE V

Run 1

Thickness 1.27 cm Dry Bulb 140   Wet Bulb 95 Relative Humidity 19%

Draft Guage   0.357 Air Velocity 600 ft/min Dry Density 0.130 g/cc

Time Mins.	Total Wt. Gms.	Total Wt. H₂O Gms.	% Free H₂O, gms H₂Ox100/gm fiber	Drying Rate gm./hr-cm²
0	452.3	230.55		0.294
5	440.3	318.55		.309
10	428.5	306.75		.304
15	417.2	295.45		.291
20	405.6	283.85		.299
25	393.6	271.85		.309
30	382.0	260.25		.299
35	370.6	248.85		.294
40	357.6	235.85		.335
45	345.7	223.95	522	.307
50	334.8	213.05	496	.281
55	323.0	201.25	469	.304
60	312.1	190.35	444	.281
65	300.9	179.15	417	.289
70	289.4	168.65	393	.271
75	278.2	157.45	366	.289
80	266.8	146.05	340	.294
85	255.5	134.75	313	.291
90	244.2	123.45	287	.291
95	232.9	112.15	261	.291
100	221.5	100.75	233	.294
105	210.4	89.65	208	.286
110	199.7	78.95	183	.276
115	189.0	68.25	158	.276
120	178.1	57.35	133	.281
125	167.9	47.15	109	.263
130	158.8	37.05	84.7	.235
135	151.3	27.55	67.2	.193
140	145.5	23.75	53.6	.150
145	141.4	19.65	44.0	.106
150	138.2	16.45	36.5	.083
155	135.5	13.75	30.2	.070
160	133.3	11.55	25.0	.057
165	131.4	9.65	20.6	.049
170	129.9	8.15	17.1	.039
175	128.6	6.85	14.0	.034
180	127.5	5.75	11.5	.028
185	126.5	4.75	9.1	.026
195	124.8	3.05	5.2	.022
205	123.6	1.85	2.3	.015
215	123.0	1.25	0.9	.008
225	122.75	1.00	0.3	.003
235	122.60	0.85	0.0	.002

TABLE VI

Run 2

Thickness 1.27 cm   Dry Bulb 140   Wet Bulb 95   Relative Humidity 19%

Draft Guage 0.557   Air Velocity 750 ft/min   Dry Density 0.130 gm/cc

Time Mins.	Total Wt. Gms.	Total Wt. H$_2$O Gms.	% Free H$_2$O, gms H$_2$Ox100/gm fiber	Drying Rate gm/hr-cm^2
0	416.8	294.85	686	0.361
5	403.0	281.05	653	.356
10	389.3	267.35	623	.353
15	375.9	253.95	591	.345
20	362.8	240.85	560	.338
25	449.7	227.75	529	.338
30	336.9	214.95	500	.330
35	323.6	201.65	470	.343
40	310.5	188.55	438	.338
45	297.3	175.35	408	.341
50	284.7	162.75	378	.325
55	271.9	149.95	348	.330
60	258.9	136.95	318	.335
65	246.4	124.45	289	.323
70	234.1	112.15	262	.317
75	221.4	99.45	230	.327
80	208.5	86.55	200	.333
85	195.7	73.75	170	.330
90	183.8	61.85	143	.307
95	173.0	51.05	120	.279
100	164.0	42.05	96.2	.232
105	157.3	35.35	80.7	.173
110	151.7	29.75	67.5	.145
115	147.8	25.85	58.3	.101
120	144.5	22.55	51.7	.085
125	141.8	19.85	44.4	.070
130	139.5	17.55	37.0	.059
135	137.5	15.55	34.3	.052
140	135.6	13.65	30.0	.049
145	133.9	11.95	25.9	.044
150	132.4	10.45	22.4	.039
155	131.1	9.15	19.4	.034
160	130.0	8.05	16.8	.028
165	128.9	6.95	14.2	.028
170	127.8	5.85	11.7	.028
180	126.0	4.05	7.5	.023
190	124.7	2.75	4.4	.017
200	123.8	1.85	2.3	.012
210	123.4	1.45	1.4	.005
220	122.9	0.95	0.2	.006
230	122.8	0.85	0.1	.001
300	122.8			

TABLE VII

Run 3

Thickness 1.27 cm Dry Bulb 140   Wet Bulb 95 Relative Humidity 19%

Draft Guage   0.800 Air Velocity 900 ft/min   Dry Density 0.130 g/cc

Time Mins.	Total Wt. Gms.	Total Wt. H_2O Gms.	% Free H_2O, gms H_2Ox100/gm fiber	Drying Rate $gm/hr-cm^2$
0	456.1	334.25		0.387
5	441.5	319.65		.377
10	427.2	305.35		.369
15	412.6	290.75		.377
20	398.0	276.15	646	.377
25	384.3	262.45	612	.354
30	370.0	248.15	579	.359
35	355.8	233.95	545	.367
40	341.6	219.75	512	.367
45	327.7	205.85	479	.359
50	313.7	191.85	447	.361
55	300.1	178.25	415	.351
60	286.2	164.35	382	.359
65	272.4	150.55	350	.356
70	259.0	137.15	319	.346
75	245.3	123.45	287	.353
80	231.9	110.05	255	.346
85	218.2	96.35	223	.354
90	205.1	83.25	193	.338
95	192.3	70.45	163	.330
100	179.3	57.45	132	.335
105	168.3	46.45	107	.284
110	160.1	38.25	87.4	.211
115	153.7	31.85	72.3	.165
120	148.8	26.95	58.8	.126
125	144.6	22.75	51.3	.108
130	141.5	19.65	44.0	.080
135	138.6	17.75	39.5	.075
140	136.0	14.15	31.1	.067
145	134.0	12.15	26.5	.052
150	132.0	10.15	21.7	.052
155	130.4	8.55	18.0	.041
160	128.9	6.05	12.2	.039
165	127.5	5.65	11.2	.036
170	126.4	4.55	8,7	.028
180	124.8	2.95	4.9	.021
190	123.8	1.95	2.6	.013
200	123.2	1.35	1.2	.008
210	122.9	1.05	0.5	.004
220	122.7	0.85	0.0	.003
300	122.7			

75

TABLE VIII

Run 4

Thickness 1.27 cm   Dry Bulb 140   Wet Bulb 95   Relative Humidity 19%

Draft Guage 0.248   Air Velocity 500 ft/min   Dry Density 0.130 g/cc

Time Mins.	Total Wt. Gms.	Total Wt. H_2O Gms.	% Free H_2O, gms H_2Ox100/gm fiber	Drying Rate gm/hr-cm^2
0	323.9	202.05	470	0.250
5	314.3	192.45	448	.247
10	304.4	182.55	425	.255
15	294.8	172.95	402	.247
20	285.1	163.25	380	.250
25	275.7	153.85	357	.242
30	266.0	144.50	335	.250
35	256.6	134.75	312	.242
40	247.0	125.15	291	.247
45	237.5	115.65	268	.245
50	228.3	106.45	247	.237
55	219.0	97.15	225	.240
60	209.9	88.05	204	.235
65	200.5	78.65	182	.242
70	191.3	69.45	162	.237
75	182.3	60.45	139	.232
80	173.3	51.45	118	.232
85	165.5	43.65	100	.201
90	159.4	37.55	85.8	.157
95	154.7	32.85	74.7	.121
100	150.8	28.95	65.8	.101
105	147.8	25.95	58.7	.077
110	145.1	23.25	52.3	.070
115	142.6	20.75	46.6	.064
120	140.5	18.65	41.6	.054
125	138.8	16.95	37.6	.044
130	137.1	15.25	33.7	.044
135	135.5	13.65	29.9	.041
140	134.0	12.15	26.4	.039
145	132.6	10.75	23.2	.036
150	131.4	9.55	20.3	.031
155	130.3	8.45	17.8	.028
160	129.2	7.35	15.2	.028
165	128.4	6.55	13.3	.021
170	127.7	5.85	11.7	.018
175	126.9	5.05	9.8	.021
185	126.0	4.15	7.7	.012
195	125.0	3.15	5.4	.013
205	124.2	2.35	3.5	.010
215	123.6	1.75	2.1	.008
225	123.2	1.35	1.2	.005
235	123.0	1.15	0.7	.003
245	122.8	0.95	0.2	.003
255	122.7	0.85	0.0	.001

TABLE IX

Run 5

Thickness 1.27 cm Dry Bulb 140 Wet Bulb 95 Relative Humidity 1%

Draft Guage 0.357 Air Velocity 600 ft/min Dry Density 0.130 g/cc

Time Mins.	Total Wt. Gms.	Total Wt. H2O Gms.	% Free H2O, gms H2Ox100/gm fiber	Drying Rate gm/hr-cm^2
0	308.0	185.45	425	0.292
5	297.0	174.45	400	.284
10	285.7	163.15	374	.292
15	274.8	153.25	351	.282
20	263.6	143.65	329	.289
25	252.8	132.25	303	.279
30	241.9	121.35	277	.281
35	231.1	110.55	253	.279
40	220.2	99.45	227	.282
45	209.5	88.95	203	.277
50	178.8	78.25	178	.277
55	188.1	67.55	153	.277
60	178.1	57.55	130	.258
65	169.2	48.65	110	.230
70	161.9	41.35	93.2	.188
75	156.5	35.95	80.9	.139
80	152.1	31.55	70.6	.113
85	148.5	27.95	62.4	.093
90	145.5	23.95	55.1	.077
95	142.8	21.25	46.8	.070
100	140.6	18.05	39.5	.057
105	138.7	16.15	35.1	.049
110	136.8	14.25	30.8	.049
115	135.3	12.75	27.3	.039
120	133.7	11.15	23.7	.041
125	132.5	9.95	21.9	.031
130	131.2	8.65	17.9	.034
135	130.3	7.75	15.8	.023
140	129.1	6.55	13.1	.031
145	128.1	5.55	10.8	.026
150	127.4	4.85	9.1	.018
155	126.6	4.05	7.3	.021
165	125.7	3.15	5.3	.012
175	125.0	2.45	3.6	.009
185	124.4	1.85	2.3	.007
195	124.0	1.45	1.3	.005
205	123.7	1.15	0.7	.004
215	123.5	0.95	0.2	.003
225	123.4	0.85	0.0	.001
300	123.4			

TABLE X

Run 6

Thickness 1.27 cm   Dry Bulb   140   Wet Bulb   95   Relative Humidity 19%

Draft Guage 0.557   Air Velocity   750 ft/min   Dry Density 0.130 g/cc

Time Mins.	Total Wt. Gms.	Total Wt. H$_2$O Gms.	% Free H$_2$O, gms H$_2$Ox100/gm fiber	Drying Rate gm/hr-cm^2	Potentio-meter, mv
0	428.2	306.45	700	0.356	
5	414.9	293.15	668	.343	
10	401.0	279.25	637	.357	
15	387.6	265.85	604	.346	
20	374.0	252.25	574	.351	
25	360.3	238.55	545	.354	
30	346.6	224.85	512	.354	
35	333.2	211.45	481	.346	
40	319.7	197.95	450	.348	
45	306.0	184.25	419	.353	
50	292.7	170.95	389	.343	1.62
55	279.4	157.65	359	.343	1.62
60	265.8	144.05	319	.351	1.62
65	252.6	130.85	297	.341	1.62
70	239.0	117.25	266	.351	1.62
75	226.4	104.65	237	.325	1.62
80	213.6	91.85	208	.330	1.62
85	200.8	79.05	179	.330	1.62
90	188.5	66.75	151	.317	1.62
95	176.3	54.55	123	.315	1.62
100	165.4	43.65	98	.281	1.62
105	157.3	35.55	81.3	.209	1.62
110	151.0	29.25	64.8	.163	1.62
115	146.7	24.95	56.4	.111	1.62
120	142.9	21.15	47.6	.098	1.62
125	139.8	18.05	40.2	.080	1.62
130	137.2	15.45	34.1	.067	1.64
135	134.9	13.15	28.8	.059	1.64
140	133.0	11.25	24.3	.049	1.64
145	131.1	9.35	19.9	.049	1.64
150	129.5	7.75	16.2	.041	1.73
155	128.0	6.25	12.6	.039	1.85
160	126.8	5.05	9.8	.067	2.01
165	125.8	4.05	7.5	.026	2.25
170	125.0	3.25	5.6	.020	2.44
175	124.25	2.50	3.9	.019	2.58
185	123.25	1.50	1.5	.013	2.72
195	122.95	1.20	0.8	.004	2.77
205	122.75	1.00	0.3	.003	2.79
215	122.60	0.85	0.0	.002	2.79
300	122.60	0.85	0.0	.000	2.79

TABLE XI

Run 7

Thickness 1.27 cm Dry Bulb 140 Wet Bulb 95 Relative Humidity 19%

Draft Guage 0.800 Air Velocity 900 ft/min Dry Density 0.130 g/cc

Time Mins.	Total Wt. Gms.	Total Wt. H₂O Gms.	% Free H₂O, gms H₂Ox100/gm fiber	Drying Rate gm/hr-cm²
0	480.0	358.05	817	0.419
5	462.8	340.85	776	.414
10	446.6	324.65	738	.419
15	429.7	307.75	716	.436
20	412.5	290.55	676	.444
25	396.2	274.25	639	.421
30	380.0	258.05	601	.419
35	363.4	241.45	561	.429
40	347.0	225.05	524	.423
45	331.0	209.05	487	.413
50	314.5	192.55	448	.426
55	298.7	176.75	410	.408
60	282.5	160.55	373	.418
65	266.0	144.05	335	.426
70	249.9	127.95	297	.416
75	233.4	111.45	259	.426
80	217.3	95.35	221	.416
85	201.3	79.35	184	.413
90	186.6	64.65	149	.380
95	173.4	51.45	118	.341
100	162.4	40.45	92.5	.284
105	154.6	32.65	74.3	.201
110	148.7	26.75	60.5	.152
115	144.5	22.55	51.7	.108
120	140.8	18.85	42.0	.096
125	137.8	15.85	35.0	.077
130	135.2	13.25	29.0	.067
135	132.8	10.85	23.3	.062
140	130.8	8.85	18.7	.052
145	129.2	7.25	14.9	.041
150	127.8	5.85	11.6	.036
155	126.7	4.75	9.1	.028
160	125.7	3.75	6.8	.026
165	124.9	2.95	4.9	.021
175	123.9	1.95	2.6	.013
185	123.3	1.35	1.1	.008
195	123.0	1.05	0.5	.004
205	122.8	0.85	0.0	.003
215	122.8	0.85	0.0	.000
300	122.8			

TABLE XII

Run 8

Thickness 1.27 cm   Dry Bulb 140   Wet Bulb 95   Relative Humidity 19%

Draft Guage 1.085   Air Velocity 1050 ft/min   Dry Density 0.130 g/cc

Time Mins.	Total Wt. Gms.	Total Wt. H_2O Gms.	% Free H_2O, gms H_2Ox100/gm fiber	Drying Rate gm/hr-cm^2
0	457.8	336.05		0.464
5	440.0	318.25	743	.459
10	421.9	300.15	700	.467
15	404.1	282.35	658	.459
20	386.1	264.35	616	.464
25	368.6	246.85	575	.452
30	350.8	229.05	534	.459
35	333.7	211.95	493	.441
40	315.9	194.15	453	.459
45	298.6	176.85	411	.446
50	281.4	159.6	372	.442
55	264.1	142.35	331	.446
60	246.9	125.15	291	.444
65	229.7	107.95	250	.444
70	212.6	90.85	210	.441
75	196.2	74.45	173	.423
80	180.9	59.15	137	.395
85	167.2	45.45	104	.354
90	157.6	35.85	81.8	.248
95	150.6	28.85	65.4	.181
100	145.6	23.85	53.7	.129
105	141.6	19.85	44.5	.103
110	138.1	16.55	36.7	.090
115	135.2	13.45	29.5	.075
120	132.6	10.85	23.4	.067
125	130.4	8.65	18.2	.057
130	128.9	7.15	16.1	.039
135	127.6	5.85	11.7	.034
140	126.3	4.55	8.7	.034
145	125.4	3.65	5.5	.023
150	124.6	2.85	4.7	.021
160	123.5	1.95	2.6	.014
170	122.9	1.15	0.7	.008
180	122.7	0.95	0.2	.003
190	122.6	0.85	0.0	.001
300	122.6	0.85	0.0	.001

TABLE XIII

Run 9

Thickness 1.27 cm   Dry Bulb 140   Wet Bulb 118   Relative Humidity 51%

Draft Guage 0.602   Air Velocity 47.3 lb/ft^2-hr   Dry Density 0.130 g/cc

Time Mins.	Total Wt. Gms.	Total Wt. H_2O Gms.	% Free H_2O, gms H_2Ox100/gm fiber	Drying Rate gm/hr-cm^2
0	265.0	143.0	330	0.193
5	257.6	135.6	313	.191
10	250.4	128.4	296	.186
15	242.9	120.9	279	.193
20	235.3	113.3	261	.196
25	228.1	106.1	244	.186
30	221.0	99.0	227	.183
35	213.8	91.8	210	.186
40	206.5	84.5	194	.188
45	199.3	77.3	177	.186
50	192.3	70.3	160	.181
55	184.9	62.9	143	.191
60	177.8	55.8	127	.183
65	170.6	48.6	110	.186
70	163.9	41.9	94.1	.173
75	158.2	36.2	81.0	.147
80	153.7	31.7	70.4	.116
85	150.1	28.1	62.0	.093
90	147.1	25.1	55.2	.077
95	144.7	22.7	49.5	.062
100	142.6	20.6	44.5	.054
105	140.8	18.8	40.4	.046
110	139.3	17.3	37.8	.039
115	137.8	15.8	34.3	.039
120	136.5	14.5	30.3	.034
125	135.3	13.3	27.6	.031
130	134.1	12.1	24.6	.031
135	133.0	11.0	22.2	.028
140	131.9	9.9	19.6	.028
145	131.0	9.0	17.5	.023
155	129.9	7.9	14.9	.014
165	128.9	6.9	12.6	.013
175	127.8	5.8	10.0	.014
185	126.9	4.9	7.9	.012
195	126.0	4.0	5.8	.012
205	125.2	3.2	4.0	.010
215	124.7	2.7	2.8	.006
225	124.3	2.3	1.9	.005
235	124.0	2.0	1.2	.004
245	123.8	1.8	0.7	.003
255	123.6	1.6	0.2	.003
265	123.5	1.5	0.0	.001
330	123.5	1.5	0.0	.000

TABLE XIV

Run 10

Thickness 1.27 cm Dry Bulb 140 Wet Bulb 104 Relative Humidity 30%

Draft Guage 0.570 Air Velocity 47.3 lb/ft^2-hr Dry Density 0.130 g/cc

Time Mins.	Total Wt. Gms.	Total Wt. H$_2$O Gms.	% Free H$_2$O,gms H$_2$Ox100/gm fiber	Drying Rate gm/hr-cm^2
0	330.5	208.55	483	0.284
5	319.7	197.75	459	.279
10	308.8	186.85	433	.281
15	297.9	175.95	408	.281
20	286.8	164.85	381	.286
25	275.8	153.85	356	.284
30	265.1	143.15	330	.276
35	254.2	132.25	306	.281
40	243.4	121.45	280	.279
45	232.6	110.65	256	.279
50	221.6	99.65	230	.284
55	210.7	88.75	204	.284
60	200.0	78.05	180	.276
65	189.2	67.25	154	.279
70	178.8	56.85	130	.268
75	170.0	48.05	110	.227
80	162.6	40.65	92.8	.191
85	156.7	34.75	78.8	.152
90	152.1	30.15	68.0	.119
95	148.1	26.15	58.7	.103
100	145.4	23.45	52.3	.070
105	142.9	20.95	46.5	.065
110	140.4	18.45	40.7	.065
115	138.5	16.55	37.2	.049
120	136.8	14.85	32.3	.044
125	135.2	13.25	28.7	.041
130	133.8	11.85	25.3	.036
135	132.5	10.55	22.2	.034
140	131.3	9.35	19.4	.031
145	130.3	8.35	17.1	.026
150	129.6	7.65	15.5	.018
155	128.5	6.55	12.9	.028
165	127.2	5.25	9.9	.017
175	126.1	4.15	7.3	.014
185	125.2	3.25	5.2	.012
195	124.6	2.65	3.8	.007
205	124.1	2.15	2.6	.006
215	123.7	1.75	1.7	.005
225	123.4	1.45	1.0	.004
235	123.1	1.15	0.3	.004
245	123.0	1.05	0.0	.001
300	123.0	1.05	0.0	.000

TABLE XV

Run 11

Thickness 1.27 cm Dry Bulb 140 Wet Bulb 100 Relative Humidity 25%

Draft Guage 0.561 Air Velocity 47.3 lb/ft^2-hr Dry Density 0.130 g/cc

Time Mins.	Total Wt. Gms.	Total Wt. H$_2$O Gms.	% Free H$_2$O,gms H$_2$Ox100/gm fiber	Drying Rate gm/hr/cm^2
0	362.2	240.0	552	0.305
5	350.3	228.1	524	.307
10	338.1	215.9	496	.315
15	326.3	204.1	469	.305
20	314.4	192.2	441	.307
25	302.8	180.6	414	.299
30	291.1	168.9	387	.302
35	279.4	157.2	361	.302
40	267.6	145.3	334	.305
45	256.1	133.9	307	.297
50	244.3	122.1	280	.305
55	232.7	110.5	253	.300
60	220.9	98.7	226	.305
65	209.3	87.1	199	.299
70	197.8	75.6	173	.297
75	186.1	63.9	145	.302
80	174.5	52.3	119	.300
85	165.2	43.0	97.2	.240
90	158.3	36.1	81.3	.178
95	152.8	30.6	68.6	.142
100	148.5	26.3	58.7	.111
105	145.0	22.8	50.6	.090
110	142.0	19.8	43.7	.077
115	139.3	17.1	37.5	.070
120	137.5	15.3	33.3	.046
125	135.7	13.5	29.2	.046
130	134.0	11.8	25.3	.044
135	132.4	10.2	21.5	.041
140	131.1	8.9	18.5	.034
145	129.8	7.6	15.5	.034
150	128.7	6.5	13.0	.028
155	127.8	5.6	10.9	.023
160	126.8	4.6	8.6	.026
170	125.7	3.5	6.1	.014
180	124.8	2.6	4.0	.012
190	124.1	1.9	2.4	.009
200	123.5	1.3	1.0	.008
210	123.2	1.0	0.3	.004
220	123.05	0.85	0.0	.002
300	123.05	0.85	0.0	.000

TABLE XVI

Run 12

Thickness 1.27 cm Dry Bulb 170 Wet Bulb 115 Relative Humidity 19%

Draft Guage 0.602 Air Velocity 47.3 lb/ft^2-hr Dry Density 0.130 g/cc

Time Mins.	Total Wt. Gms.	Total Wt. H$_2$O Gms.	% Free H$_2$O, gms H$_2$Ox100/gm fiber	Drying Rate gm/hr-cm^2
0	449.5	327.1	754	0.451
5	432.7	310.3	714	.433
10	416.0	293.6	677	.431
15	398.0	275.6	635	.464
20	381.3	258.9	597	.430
25	364.7	242.3	588	.428
30	347.4	225.0	519	.446
35	330.2	207.8	478	.443
40	312.5	190.1	438	.456
45	295.3	172.9	390	.444
50	279.2	156.8	360	.415
55	262.2	139.8	322	.438
60	246.0	123.6	284	.417
65	230.0	107.6	247	.412
70	213.2	90.8	208	.433
75	198.4	76.0	174	.382
80	183.3	60.9	140	.389
85	169.8	47.4	108	.348
90	159.2	36.8	83.8	.273
95	152.0	29.6	67.1	.186
100	146.7	24.3	55.0	.137
105	142.5	20.1	45.2	.108
110	139.2	16.8	37.6	.085
115	136.3	13.9	30.9	.075
120	133.9	11.5	25.4	.062
125	131.8	9.4	20.5	.054
130	130.0	7.6	16.3	.046
135	128.4	6.0	12.7	.041
140	126.9	4.5	9.2	.039
145	125.8	3.4	6.6	.028
150	125.0	2.6	4.8	.021
160	123.7	1.3	1.8	.017
170	123.2	0.8	0.6	.006
180	123.0	0.6	0.2	.003
190	122.9	0.5	0.0	.001
200	122.9	0.5	0.0	.000

TABLE XVII

Run 13

Thickness 1.27 cm Dry Bulb 200 Wet Bulb 135 Relative Humidity 19%

Draft Guage 0.707 Air Velocity 47.3 lb/ft^2-hr Dry Density 0.130 g/cc

Time Mins.	Total Wt. Gms.	Total Wt. H$_2$O Gms.	% Free H$_2$O, gms H$_2$Ox100/gm fiber	Drying Rate gm/hr-cm^2
0	505.0	383.0	892	0.420
5	482.9	360.9	840	.569
10	463.2	341.2	795	.508
15	443.5	321.5	748	.508
20	421.0	299.0	696	.579
25	399.5	277.5	646	.554
30	380.2	258.2	600	.497
35	358.4	236.4	550	.562
40	337.5	215.5	501	.539
45	316.3	194.3	453	.546
50	296.3	174.3	405	.516
55	274.0	152.0	353	.574
60	254.8	132.8	308	.494
65	233.3	111.3	258	.555
70	212.2	91.3	212	.544
75	192.2	70.2	163	.515
80	174.6	52.6	122	.453
85	160.4	38.4	88.9	.366
90	152.0	30.0	69.3	.217
95	145.4	23.4	53.9	.170
100	141.1	19.1	43.8	.111
105	137.2	15.2	34.4	.101
110	134.1	12.1	27.6	.080
115	131.6	9.6	21.7	.064
120	129.3	7.3	16.4	.059
125	127.5	5.5	12.2	.046
130	126.0	4.0	8.7	.039
135	124.6	2.6	5.4	.036
140	123.9	1.9	3.8	.018
145	123.5	1.5	2.9	.010
150	123.1	1.1	1.9	.010
155	122.8	0.9	1.4	.005
160	122.5	0.5	0.5	.008
165	122.3	0.3	0.0	.005
170	122.3	0.3	0.0	.000
240	122.3	0.3	0.0	.000

TABLE XVIII

Run 14

Thickness 2.54 cm Dry Bulb 140 Wet Bulb 95 Relative Humidity 19%

Draft Guage 0.557 Air Velocity 47.3 lb/ft^2-hr Dry Density 0.130 g/cc

Time Mins.	Total Wt. Gms.	Total Wt. H$_2$O Gms.	% Free H$_2$O,gms H$_2$Ox100/gm fiber	Drying Rate gm/hr-cm^2
0	575.6	354.4	412	.361
5	562.0	340.8	396	.357
10	548.6	327.4	380	.346
15	535.4	314.2	365	.341
20	522.0	300.8	349	.345
25	508.4	287.2	333	.351
30	494.9	273.7	318	.348
35	481.9	260.7	302	.335
40	468.5	247.3	287	.345
45	455.4	234.2	271	.338
50	442.2	221.0	257	.341
55	428.7	207.5	241	.348
60	415.9	194.7	226	.330
65	403.2	182.0	210	.327
70	390.1	168.9	195	.338
75	377.1	155.9	180	.335
80	364.2	143.0	165	.333
85	351.5	130.3	150	.327
90	339.7	118.5	137	.304
95	328.2	107.0	123	.297
100	317.7	96.5	111	.271
105	308.4	87.2	100	.240
110	300.8	79.6	91.1	.196
115	293.6	72.4	82.6	.186
120	288.2	67.0	76.3	.139
125	283.3	62.1	70.6	.127
130	279.3	58.1	65.9	.103
135	275.6	54.4	61.5	.096
140	272.4	51.2	57.8	.083
145	269.4	48.2	54.4	.072
150	266.6	45.4	51.1	.072
155	264.2	43.0	48.3	.062
160	261.8	40.6	45.4	.062
165	259.8	38.6	43.1	.052
170	257.7	36.5	40.6	.054
175	256.1	34.9	38.8	.041
180	254.0	32.8	36.3	.054
185	252.2	31.0	34.2	.046
190	250.7	29.5	32.5	.039
195	249.2	28.0	30.7	.039
200	247.8	26.6	29.0	.036
205	246.5	25.3	27.6	.034
210	245.2	24.0	26.0	.034

TABLE XVIII, Run 14 Continued

Time Mins.	Total Wt. Gms.	Total Wt. H_2O Gms.	% Free H_2O,gms H_2Ox100/gm fiber	Drying Rate gm/hr-cm^2
215	244.0	22.8	24.7	0.031
220	242.8	21.6	23.2	.031
225	241.5	20.3	21.7	.034
230	240.3	19.1	20.3	.031
235	239.1	17.9	18.9	.031
240	237.8	16.6	17.4	.034
250	235.9	14.7	15.2	.025
260	234.2	13.0	13.2	.022
270	232.7	11.5	11.4	.019
280	231.3	10.1	9.8	.018
290	229.8	8.6	8.0	.019
300	228.7	7.5	6.8	.014
310	227.6	6.4	5.5	.014
320	226.6	5.4	4.3	.013
330	225.9	4.7	3.5	.009
340	225.0	3.8	2.4	.012
350	224.4	3.2	1.7	.008
360	223.8	2.6	0.8	.008
370	223.3	2.1	0.5	.006
380	223.0	1.8	0.1	.004
390	222.9	1.7	0.0	.001
420	222.9	1.7	0.0	.000

TABLE XIX

Run 15

Thickness 0.635 cm Dry Bulb 140 Wet Bulb 95 Relative Humidity 19%

Draft Guage 0.557 Air Velocity 47.3 lb/ft^2-hr Dry Density 0.130 g/cc

Time Mins.	Total Wt. Gms.	Total Wt. H_2O Gms.	% Free H_2O,gms H_2Ox100/gm fiber	Drying Rate gm/hr-cm^2
0	271.0	203.55	946	0.345
5	257.5	190.05	885	.348
10	243.8	176.35	820	.353
15	230.2	162.75	756	.353
20	216.8	149.35	694	.345
25	203.3	135.85	631	.348
30	189.7	122.25	568	.351
35	176.7	109.25	507	.335
40	163.4	95.95	446	.343
45	149.8	82.35	382	.351
50	136.5	69.05	319	.343
55	123.3	55.85	258	.340
60	110.2	42.75	197	.338
65	97.4	29.95	137	.330
70	86.5	19.05	86.3	.281
75	79.4	11.95	53.4	.183
80	75.2	7.75	34.0	.108
85	72.1	4.65	19.6	.080
90	69.9	2.45	9.4	.057
95	68.8	1.35	4.3	.028
100	68.1	0.65	1.0	.018
105	68.0	0.55	0.0	.003
180	68.0	0.55	0.0	.000

TABLE XX

Run 16

Thickness 1.27 cm Dry Bulb 140 Wet Bulb 100 Relative Humidity 25%

Draft Guage 0.561 Air Velocity 47.3 lb/ft^2-hr Dry Density 0.152 g/cc

Time Mins.	Total Wt. Gms.	Total Wt. H_2O Gms.	% Free H_2O,gms H_2Ox100/gm fiber	Drying Rate gm/hr-cm^2
0	304.1	174.2	346	0.307
5	292.1	162.2	323	.309
10	280.4	150.5	299	.301
15	268.6	138.7	274	.304
20	256.9	127.0	252	.301
25	245.6	115.7	229	.291
30	234.1	104.2	207	.297
35	222.2	92.3	182	.307
40	210.3	80.4	159	.307
45	200.3	70.4	139	.258
50	191.9	62.0	122	.217
55	183.8	53.9	105	.209
60	176.5	46.6	90.4	.188
65	170.5	40.6	78.4	.155
70	165.7	35.8	68.7	.124
75	161.5	31.6	60.5	.108
80	158.2	28.3	53.8	.085
85	155.3	25.4	48.0	.075
90	152.8	22.9	43.0	.064
95	150.6	20.7	38.6	.057
100	148.5	18.6	34.3	.054
105	146.7	16.8	30.8	.046
110	145.0	15.1	27.4	.044
115	143.5	13.6	24.3	.039
120	142.1	12.2	21.6	.036
125	140.8	10.9	19.0	.034
130	139.7	9.8	16.7	.028
140	137.6	7.7	12.5	.027
150	135.8	5.9	8.9	.023
160	134.5	4.6	6.4	.017
170	133.5	3.6	4.3	.013
180	132.6	2.7	3.1	.012
190	131.9	2.0	1.8	.009
200	131.4	1.5	0.8	.006
210	131.1	1.2	0.2	.004
220	131.0	1.1	0.0	.001
300	131.0	1.1	0.0	.000

TABLE XXI

Run 17

Thickness 1.27 cm   Dry Bulb 140   Wet Bulb 100   Relative Humidity 25%

Draft Guage 0.561   Air Velocity 47.3 lb/ft^2-hr   Dry Density 0.160 g/cc

Time Mins.	Total Wt. Gms.	Total Wt. H$_2$O Gms.	% Free H$_2$O,gms H$_2$Ox100/gm fiber	Drying Rate gm/hr-cm^2
0	351.8	221.7	424	0.317
5	339.8	209.9	401	.309
10	328.2	178.3	380	.299
15	315.7	186.0	356	.322
20	303.1	173.2	331	.326
25	291.1	161.2	308	.309
30	278.9	149.0	285	.315
35	266.5	136.6	261	.320
40	255.1	125.2	240	.295
45	243.5	113.6	216	.299
50	231.9	102.0	194	.299
55	220.9	91.0	173	.284
60	210.0	80.1	152	.281
65	200.8	70.9	134	.237
70	190.5	60.6	115	.266
75	182.2	52.3	99.0	.214
80	175.4	45.5	85.5	.175
85	169.8	37.9	74.7	.145
90	165.1	35.2	65.7	.121
95	161.3	31.4	58.4	.098
100	158.1	28.2	52.1	.083
105	155.4	25.5	47.0	.070
110	153.0	23.1	42.4	.062
115	150.9	21.0	38.4	.054
120	148.8	18.9	34.3	.054
125	147.1	17.2	31.2	.044
130	145.3	15.4	27.4	.046
135	143.9	14.0	24.9	.036
140	142.4	12.5	22.0	.037
145	141.3	11.4	19.7	.028
150	140.0	10.1	17.4	.032
155	138.9	9.0	15.3	.028
160	138.1	8.2	13.8	.021
165	137.1	7.2	11.8	.026
175	135.4	5.5	8.6	.017
185	134.1	4.2	5.1	.017
195	133.1	3.2	4.1	.013
205	132.3	2.4	2.6	.010
215	131.7	1.8	1.5	.008
225	131.3	1.4	0.7	.005
235	131.0	1.1	0.2	.004
245	130.9	1.0	0.0	.001
255	130.9	1.0	0.0	.000

TABLE XXII

Run 18

Thickness 1.27 cm Dry Bulb 140 Wet Bulb 95 Relative Humidity 19%

Draft Guage 0.557 Air Velocity 47.3 lb/ft^2-hr Dry Density 0.110 g/cc

Time Mins.	Total Wt. Gms.	Total Wt. H$_2$O Gms.	% Free H$_2$O,gms H$_2$Ox100/gm fiber	Drying Rate gm/hr-cm^2
0	392.1	276.95	761	.358
5	378.1	262.95	723	.361
10	364.2	249.05	685	.358
15	350.3	235.15	647	.358
20	336.4	221.25	608	.358
25	323.1	207.95	571	.343
30	309.4	194.25	534	.353
35	296.0	180.85	497	.345
40	282.0	166.85	458	.361
45	268.8	153.65	422	.340
50	255.4	140.25	385	.345
55	241.8	126.65	347	.351
60	227.9	112.75	309	.358
65	215.0	99.85	273	.333
70	201.5	86.35	236	.348
75	188.5	73.35	200	.335
80	175.5	60.35	165	.335
85	163.5	48.35	131	.309
90	152.8	37.65	102	.276
95	144.8	29.65	79.8	.207
100	139.2	24.05	64.3	.145
105	134.7	19.75	52.4	.111
110	131.5	16.35	43.1	.088
115	128.7	13.55	35.4	.072
120	126.1	10.95	28.2	.067
125	124.3	9.15	23.3	.046
130	122.5	7.35	18.3	.046
135	121.1	5.95	14.4	.036
140	120.2	5.05	11.9	.023
145	119.1	3.95	8.9	.028
150	118.3	3.15	5.7	.021
155	117.7	2.55	5.0	.015
160	117.2	2.05	3.7	.013
165	117.0	1.85	3.1	.005
175	116.4	1.25	1.5	.008
185	116.1	0.95	0.6	.004
195	115.9	0.75	0.0	.003
205	115.9	0.75	0.0	.000
300	115.9	0.75	0.0	.000

TABLE XXIII

Run 19

Thickness 1.27 cm Dry Bulb 140 Wet Bulb 95 Relative Humidity 19%

Draft Guage 0.557 Air Velocity 47.3 lb/ft^2-hr Dry Density 0.232 g/cc

Time Mins.	Total Wt. Gms.	Total Wt. H_2O Gms.	% Free H_2O,gms H_2Ox100/gm fiber	Drying Rate gm/hr-cm^2
0	496.2	341.1	446	0.382
5	482.6	327.5	428	.351
10	469.4	314.3	410	.341
15	456.0	300.9	393	.345
20	443.2	288.1	376	.330
25	430.3	275.2	359	.333
30	417.3	262.2	344	.335
35	404.7	249.6	325	.325
40	392.1	237.0	309	.325
45	379.5	224.4	293	.325
50	367.2	212.1	278	.317
55	355.1	200.0	261	.312
60	342.9	187.8	245	.315
65	330.8	175.7	229	.312
70	318.7	163.6	203	.312
75	307.0	151.9	197	.301
80	295.0	139.9	184	.309
85	283.3	128.2	166	.302
90	272.0	116.9	151	.292
95	261.3	106.2	138	.276
100	251.3	96.2	124	.258
105	241.9	86.8	112	.243
110	233.3	78.2	100	.222
115	225.7	70.6	90.6	.196
120	218.8	63.7	81.6	.178
125	213.1	58.0	74.1	.147
130	208.3	53.2	67.9	.124
135	204.1	49.0	62.3	.108
140	200.7	45.6	57.9	.088
145	197.6	42.5	53.8	.080
150	194.9	39.8	50.2	.070
155	192.5	37.4	47.1	.062
160	190.2	35.1	44.0	.059
165	188.0	32.9	41.1	.057
170	186.1	31.0	38.7	.049
175	184.4	29.3	36.5	.044
180	182.5	27.4	34.0	.049
195	180.9	25.8	31.8	.041
200	179.4	24.3	29.9	.039
205	177.9	22.8	27.9	.039
210	176.6	21.5	26.2	.034
215	175.3	20.2	24.5	.034

TABLE XXIII, Run 1y Continued

Time Mins.	Total Wt. Gms.	Total Wt. H2O Gms.	% Free H2O,gms H2Ox100/gm fiber	Drying Rate gm/hr-cm²
220	174.1	19.0	23.0	0.031
225	172.9	17.8	21.3	.031
230	171.8	16.7	19.9	.028
235	170.7	15.6	18.5	.028
240	169.7	14.6	17.2	.026
245	168.7	13.6	15.8	.026
250	167.6	12.5	14.4	.028
255	166.7	11.6	13.2	.023
260	165.7	10.6	11.9	.026
265	164.8	9.7	10.7	.023
270	164.0	8.9	9.7	.021
275	163.3	8.2	8.8	.018
280	162.6	7.5	7.8	.018
290	161.3	6.2	7.1	.017
300	160.2	5.1	4.7	.014
310	159.4	4.3	3.6	.010
320	158.6	3.5	2.6	.010
330	158.0	2.9	1.8	.008
340	157.5	2.4	1.1	.006
350	157.1	2.0	0.6	.005
360	156.8	1.7	0.2	.004
370	156.65	1.55	0.0	.002
280	156.65	1.55	0.0	.000
360	156.65	1.55	0.0	.000

TABLE XXIV

Run 20

Thickness 1.27 cm Dry Bulb 140 Wet Bulb 110 Relative Humidity 38%

Draft Guage 0.579 Air Velocity 47.3 lb/ft^2-hr Dry Density 0.130 g/cc

Time Mins.	Total Wt. Gms.	Total Wt. H$_2$O Gms.	% Free H$_2$O,gms H$_2$Ox100/gm fiber	Drying Rate gm/hr-cm^2
0	413.6	291.7	675	0.265
5	403.5	281.6	652	.261
10	392.8	270.9	627	.276
15	382.1	260.2	601	.276
20	371.3	249.4	576	.279
25	361.0	239.1	553	.266
30	350.1	228.2	528	.281
35	340.4	218.5	504	.250
40	330.9	209.0	483	.245
45	321.2	199.3	460	.250
50	310.7	188.8	436	.271
55	299.7	177.8	410	.283
60	289.5	167.6	386	.263
65	279.6	157.7	364	.255
70	269.9	148.0	341	.250
75	259.5	137.6	316	.268
80	249.1	127.2	293	.268
85	238.4	116.5	268	.276
90	228.2	106.3	244	.263
95	217.6	95.7	220	.273
100	207.5	85.6	196	.261
105	197.7	75.8	173	.253
110	187.7	65.8	150	.258
115	177.7	55.8	127	.258
120	168.8	46.9	106	.229
125	161.0	39.1	88.2	.201

Steam pressure caused rest of data to be erratic

CONTROLLER AND RECORDER

DRAFT GUAGE

MOTOR AND VARI-ABLE SPEED TRANS MISSION

REMOVABLE SECTIONS FOR CONTROLLING AIR FLOW

WET BULB DRY BULB

DAMPER

AIR

BLOWER

DRYING CHAMBER

MOVABLE TUBES FOR MEASURING AIR VELOCITY

MOVABLE PANEL FOR DIRECTING FLOW

STEAM RADIATOR

SCALE

AIR

DAMPER
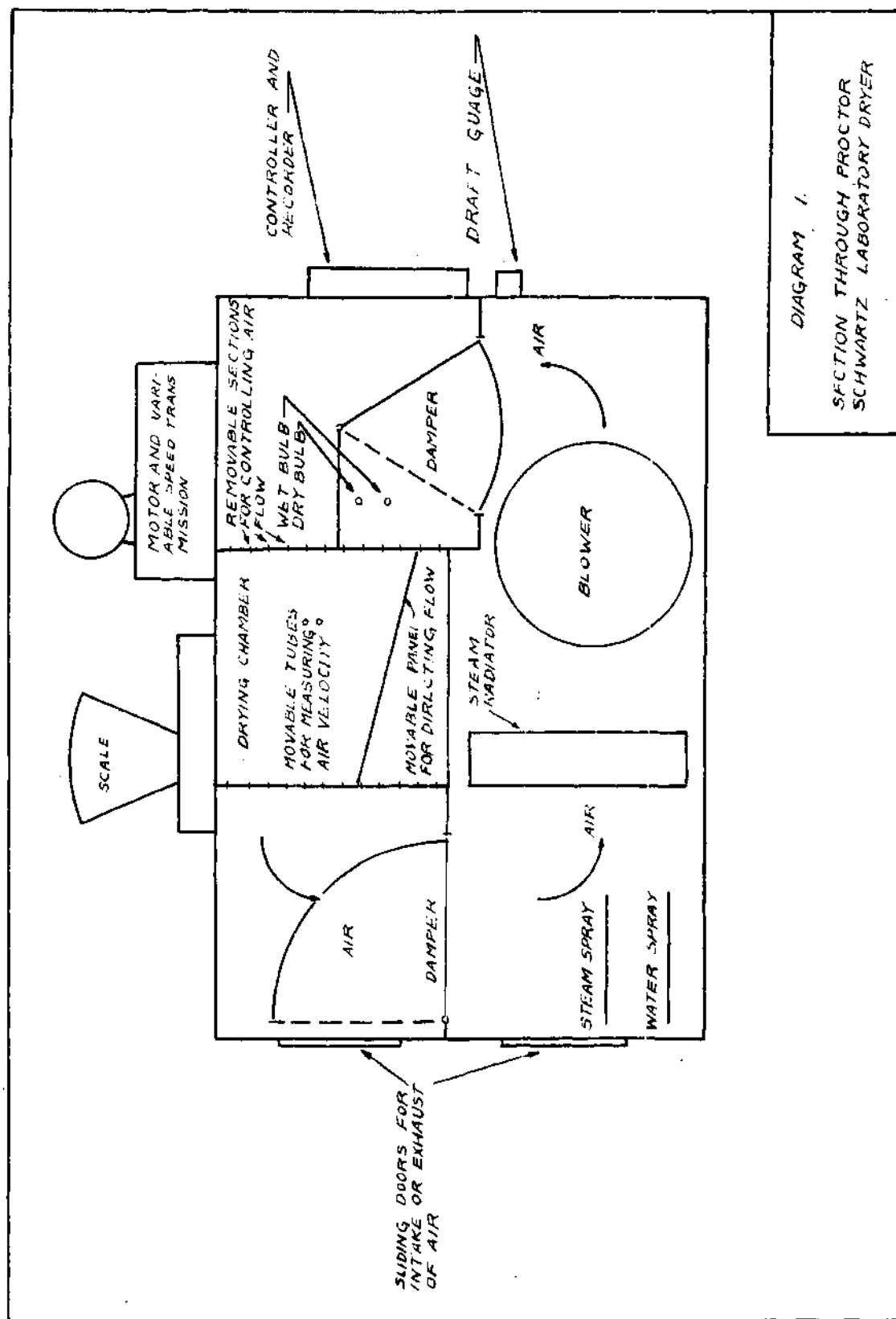
STEAM SPRAY

AIR

WATER SPRAY

SLIDING DOORS FOR INTAKE OR EXHAUST OF AIR

DIAGRAM 1.

SECTION THROUGH PROCTOR SCHWARTZ LABORATORY DRYER

DIAGRAM 2
SCHEMATIC FLOW DIAGRAM
OF PROCTOR SCHWARTZ DRYER.